Title
Exploiting animal toxins to probe molecular mechanisms of pain

Permalink
https://escholarship.org/uc/item/4rm0n56p

Author
Zhang, Chuchu

Publication Date
2017

Peer reviewed|Thesis/dissertation

EXPLOITING ANIMAL TOXINS TO PROBE MOLECULAR
MECHANISMS OF PAIN

by

Chuchu Zhang

DISSERTATION

Submitted in partial satisfaction of the requirements for the degree of

DOCTOR OF PHILOSOPHY

in

Neuroscience

in the

GRADUATE DIVISION

of the

UNIVERSITY OF CALIFORNIA, SAN FRANCISCO

Acknowledgement

The past five years have been a tremendous period of growth for me. It would never have happened without the support and care from many scientists, friends and family. I would first like to express my deep gratitude towards my mentor David Julius. His rigor with scientific inquiry and pursuit of truth has forever shaped my approach to science. His creativity and insight for science will always inspire me to explore boldly, yet reflect what is truly important. He is not only a mentor in science, but also a role model of righteousness, kindness, patient and honesty in every aspects of life that I strive to emulate. His advice, support and understanding have been critical for my personal growth. I truly feel fortunate to work with David all these years.

I also want to thank my committee members – Allan Basbaum, Robert Edwards and Diana Bautista – for their generous support and advice. They all pushed me to think about my project from different angels of their expertise and their guidance improved the quality of the work. Allan is not only the chair of my committee but also my collaborator. His extensive knowledge of pain physiology and expertise in animal behaviors are a constant source of inspiration for many interesting experiments. In addition, his sense of humor adds to our interactions that I have always enjoyed.

My fellow labmates are one of the major reasons why my experience here is so wonderful. David has fostered a productive and collaborative culture and I have learned so much from everyone around me. Elena Gracheva mentored me while I was in rotation. She is one of the most careful, thorough and vigorous scientists I have seen. She helped me form better habits for doing science, which I will benefit throughout my

Yishu Yang who I have the fortune to see the world with; Ambre Bertholet and Hye Young Lee who are both best friends and excellent female scientists models. And David Arrington, for his love, understanding and support.

Finally, I want to pay my greatest gratitude towards my parents. Ever since I have left home in China, they have been supporting my every decision with trust, warmth and faith. They encourage me during difficult times and they are always proud of me no matter what. I could never have the privilege to be here without their love.

Contributions

Part of the work was done in collaboration with other authors. In Chapter 3, Katalin F. Medzihradszky performed mass spectrometry measurements and determined partial protein sequences. Elda E. Sánchez provided snake venom and tissue. In Chapter 4, Eivind A.B. Undheim collected, fractionated centipede venoms and conducted mass spectrometry experiments. Thomas Durek did toxin synthesis. Thomas S. Dash, Peta J. Harvey and Thomas Durek conducted NMR structural analysis. All other work was done by Chuchu Zhang.

The work in Chapter 3 has been accepted for publication in the Proceedings of the National Academy of Sciences and is reproduced with permission.

Zhang, C., K. F. Medzihradszky, E. E. Sánchez, A. I. Basbaum, D. Julius (2017). "Lys49 myotoxin from the Brazilian lancehead pit viper elicits pain through regulated ATP release." Proc Natl Acad Sci U S A. DOI: 10.1073/pnas. 1615484114

EXPLOITING ANIMAL TOXINS TO PROBE MOLECULAR MECHANISMS OF PAIN

by Chuchu Zhang

ABSTRACT

Venoms from spiders, snakes, cone snails and scorpions have evolved to produce a vast pharmacopoeia of toxins that modulate receptor or channel function as a means of producing shock, hemolysis, paralysis and pain. As such, venoms from these animals represent a rich potential source of potent and selective toxins that can be exploited to study and manipulate somatosensory and nociceptive signaling pathways. In this work, I have identified and characterized two novel toxins from the Brazilian lancehead pit viper (*Bothrops moojeni*) and Tanzania blue ringleg centipede (*Scolopendra morsitans*). The Brazilian lancehead snake venom contains a novel secreted phospholipase A2 (sPLA2)-like protein that can promote ATP release from pannexin hemichannels. Studies on the cellular and behavioral effects of this toxin reveal a role of regulated endogenous nucleotide release in nociception. The discovered Tanzania blue ringleg centipede toxin represents a new family of toxins that show evolutionary relationship with α-scorpion toxins and could potentially function as potassium channel blockers.

Table of Contents

List of Figures

CHAPTER 1

Introduction

Nociception and Venom

Pain is essential to an animal's survival. Painful stimuli (mechanical, thermal, or chemical) are detected by subpopulations primary afferent sensory nerve fibers that innervate peripheral targets (Julius and Basbaum 2001, Basbaum, Bautista et al. 2009). The cell bodies of these nociceptive fibers are located in the dorsal root ganglia (DRG) or trigeminal ganglia (TG) that project to the dorsal horn of the spinal cord or brain stem, respectively (Basbaum and Jessell 2000). Somatosensory fibers can be divided into different classes that contribute to the detection of distinct pain modalities. For example, fast conducting, large diameter Aβ fibers are mainly responsible for detecting light (innocuous) touch; fast conducting, medium diameter Aδ fibers and slow conducting, small diameter C fibers are mainly detecting noxious mechanical and thermal stimuli, respectively (Basbaum, Bautista et al. 2009, Osteen, Herzig et al. 2016). One of the key mechanisms for the differential detection of somatosensory modalities is the expression of functional receptors and ion channels that can be gated by different somatosensory stimuli, such as the heat-activated TRPV1 channel, the cold-activated TRPM8 channel (Bautista, Siemens et al. 2007) and mechanically-activated Piezo channels (Coste, Mathur et al. 2010). Hence, studies of ion channels and receptors in somatosensory neurons provide a molecular framework for understanding peripheral mechanism of pain detection, sensitization and psychophysical encoding (Woolf and Ma 2007, Patapoutian, Tate et al. 2009, Julius 2013).

Animal venoms that contain predominately proteinaceous toxins have evolved to contain pharmocophores that ward off predators by generating discomfort or pain sensation in the offending species. Some of these pain-producing toxins induce ubiquitous cell damage and tissue injury, but some can also directly activate ion channels and receptors involved in the endogenous pain detection pathways (Chahl and Kirk 1975, Basbaum, Bautista et al. 2009). As such, toxins can be used as powerful tools for characterizing and manipulating existing or novel pain pathways, and for probing ion channel biophysical properties. For example, the spider-derived vanillotoxins, VaTx1-3 (Siemens, Zhou et al. 2006) and DkTx (Bohlen, Priel et al. 2010) target TRPV1 channels as one of the main pain-producing effects in these spider venoms. Structural analysis of DkTx in complex with TRPV1 revealed key gating mechanisms of this channel (Cao, Liao et al. 2013), demonstrating the power of such toxins for mechanistic studies.

Moreover, toxins are also uniquely important for understanding the evolution of venomous animals. The venom system provides unparalleled models for molecular evolution and protein neofunctionalization, as well as prey-predator interactions and natural selection (Fry, Roelants et al. 2009, Casewell, Wuster et al. 2013). Also, evolutionarily important toxins offer insights into drug design and discovery, which have already led to the development of successful pharmaceuticals (Vetter, Davis et al. 2011). However, despite the diversity of venomous animals and their toxins, much of the chemical diversity encoded within animal venoms remains uncharacterized.

In this work, my goal was to further explore this venom space to identify novel pharmocophores that could be used to study pain pathways. I have hence discovered two unique toxin families: BomoTx, a PLA$_2$-like toxin from the snake Brazilian lancehead (*Bothrops moojeni*) and SmTx1-2, a cysteine-stabilized αβ (CSαβ) fold toxin from the centipede (*Scolopendra morsitan*). Characterization of BomoTx and its signaling pathways reveal new pain mechanisms involving purinergic receptors and pannexin hemichannels. In addition, both studies demonstrate unique molecular evolution strategies in snakes and centipedes.

Snake PLA$_2$ and PLA$_2$-like toxins

Snake venoms contain a complex mixture of toxins such as metalloproteinases (Bernardes, Santos-Filho et al. 2008), serine proteases (de Oliveira, de Sousa et al. 2016), L-amino acid oxidases (LAAOs) (Franca, Kashima et al. 2007) and phospholipase A$_2$s (PLA$_2$) (Silveira, Marchi-Salvador et al. 2013) that likely contribute to different local and systemic symptoms upon envenomation. PLA$_2$s are enzymes that hydrolyze glycerophospholipids at the sn-2 position of the glycerol backbone releasing lysophosphatidic and arachidonic acids, which are precursors of inflammatory mediators. They are the most abundant and diverse components of snake venoms (Gutierrez and Lomonte 2013) that have evolved from a highly conserved structural scaffold (Wery, Schevitz et al. 1991, Chakraborti 2003). The diversity of PLA$_2$ proteins is achieved through a mechanism of gene duplication and accelerated molecular

4

evolution, in which the protein-coding regions of these PLA$_2$ genes evolve at greater substitution rates than their introns, thus allowing for acquisition of diverse toxin functions (Nakashima, Ogawa et al. 1993).

Indeed, PLA$_2$–like toxins exert a variety of physiologic and pharmacological effects, including neurotoxic, myotoxic, hemolytic, hypotensive and anticoagulant activities (Strong, Goerke et al. 1976, Gutierrez and Lomonte 1995, Rigoni, Caccin et al. 2005, Gutierrez and Lomonte 2013, Silveira, Marchi-Salvador et al. 2013). The different functions of PLA$_2$s indicate that PLA$_2$ toxicities may require more than just the enzymatic function. In fact, it has been hypothesized that PLA$_2$ toxins contain "pharmacological regions" that determine their affinity and selectivity for cellular targets (Condrea, Fletcher et al. 1981, Kini and Evans 1989, Lambeau, Schmid-Alliana et al. 1990, Lambeau and Lazdunski 1999, Valentin and Lambeau 2000, Gutierrez and Lomonte 2013), in addition to catalytic regions. Hence, it is possible that PLA$_2$ toxins could function through specific, catalytically-independent processes involving cell type recognition.

In support of this theory has been the identification of PLA$_2$ toxins that lack enzymatic activities due to the mutation of His48 or/and Asp49, which are calcium binding sites required for the catalytic process. These mutated PLA$_2$ toxins, or PLA$_2$-like toxins, exhibit target binding ability and toxicity despite complete lack enzymatic activity (Ward, Chioato et al. 2002). For example, the Texas coral snake produces a PLA$_2$-like toxin

(MitTx-β), which forms heterodimers with a Kunitz-type protein subunit (MitTx-α), which together target ASIC1 ion channels to massively potentiate proton-evoked responses by these channels, thus activating a subset of somatosensory neurons to elicit inflammatory pain (Bohlen, Chesler et al. 2011).

Lys49 myotoxins

Another family of PLA_2-like toxins, the "Lys49 myotoxins" (Maraganore, Merutka et al. 1984), has evolved within the viperid snakes and has been studied for their intriguing effects on skeletal muscle cells (Lomonte and Rangel 2012). As will be discussed in Chapter 3 in greater detail, these toxins belongs to the Lys49 myotoxin family and share a common feature wherein a Lys residue replaces the conserved Asp49 residue in the key calcium-binding site, hence abolishing the calcium-dependent catalytic properties (Ward, Chioato et al. 2002). However, despite their inability to hydrolyze phospholipids, these toxins all can damage myotubes and induce myonecrosis locally when injected intramuscularly in rodents (Gutierrez, Lomonte et al. 1986, Fernandez, Caccin et al. 2013). Consistent with this, human victims of *Bothrops* snakebites, in which Lys49 myotoxins are major components (Lomonte and Rangel 2012), often show robust pain and skeletal muscle necrosis that frequently leads to permanent tissue loss and disability (Nishioka Sde and Silveira 1992, Nishioka, Silveira et al. 2000).

Many studies have sought to understand the mechanisms of catalytically-independent muscle damaging activities of Lys49 myotoxins. It has been observed that intracellular

Ca^{2+} increase and ATP release are involved in muscle cell responses to these toxins (Cintra-Francischinelli, Caccin et al. 2010). One model supports a direct membrane disruption mechanism via the C-terminal region of Lys49 myotoxins, as heparins binding to this region inhibit myotoxicity, while synthetic peptides corresponding to this region cause Ca^{2+} entry and myotube death (Cintra-Francischinelli, Pizzo et al. 2010, Fernandes, Borges et al. 2014). However, this model does not explain why specific toxin activities are seen in skeletal muscles or differentiated myotubes, but not in undifferentiated myoblasts (Lomonte, Angulo et al. 1999, Cintra-Francischinelli, Pizzo et al. 2009). In addition, these synthetic peptides were used at very high concentrations that may produce non-physiologic events. Another model proposes that a specific membrane "receptor" is required (Tonello, Simonato et al. 2012, Giannotti, Leiguez et al. 2013, Moreira, de Castro Souto et al. 2013). This is consistent with previous discoveries that many PLA$_2$s can bind to specific membrane proteins (Gutierrez and Lomonte 2013). Indeed, efforts have been made to find membrane targets of Lys49 myotoxins (Lambeau and Lazdunski 1999) but the identity of such receptors remains elusive (Lomonte and Rangel 2012).

ATP Release and Purinergic Signaling

One of the key observations about Lys49 myotoxins, including BomoTx (see below), is their ability to induce ATP release from C2C12 myotubes (Cintra-Francischinelli, Caccin et al. 2010, Tonello, Simonato et al. 2012). Although ATP release from compromised cell membranes in injury conditions is widely accepted, evidence supporting regulated

ATP release pathways also exists. These include exocytosis of ATP-containing vesicles, often with other classic neurotransmitters (Khakh 2001, Pankratov, Lalo et al. 2006, Sawada, Echigo et al. 2008), and channel-mediated ATP release (Rabasseda, Solsona et al. 1987, Arcuino, Lin et al. 2002, Dahl 2015). Hemichannels of gap junction proteins, namely pannexins and connexins, have been shown to conduct ATP currents and are hence ATP-releasing channels (Bao, Locovei et al. 2004, MacVicar and Thompson 2010). Hemichannel-mediated ATP release has been reported in a few different cell types such as glia cells (Cotrina, Lin et al. 2000, Zhang, Chen et al. 2007), fibroblasts (Pinheiro, Paramos-de-Carvalho et al. 2013, Pinheiro, Paramos-de-Carvalho et al. 2013) and lung epithelial cells (Seminario-Vidal, Kreda et al. 2009, Seminario-Vidal, Okada et al. 2011). In these examples, pannexins can be activated by several physiological stimuli including caspase activation (Chekeni, Elliott et al. 2010), Rho signaling (Seminario-Vidal, Okada et al. 2011) and mechanical stretch (Bao, Locovei et al. 2004). Whether Lys49 myotoxins promote ATP release through such mechanisms remained to be determined.

ATP is a major signaling molecule released during tissue damage and inflammation. It can directly activate primary afferent nerve endings expressing P2X receptors to cause pain (Lewis, Neidhart et al. 1995, Bland-Ward and Humphrey 1997, North 2002). These mainly include $P2X_2$ and $P2X_3$ receptors that are expressed by C and Aδ fibers (North 2002, Staikopoulos, Sessle et al. 2007). Genetic and pharmacologic studies have demonstrated that $P2X_3$ receptors expressed on C fibers are important for the ATP-

evoked acute pain, while activation of capsaicin-insensitive P2X$_{2/3}$ primary afferent neurons, likely representing Aδ fibers, are critical for mechanical allodynia (Cockayne, Hamilton et al. 2000, Tsuda, Koizumi et al. 2000, Honore, Kage et al. 2002, Cockayne, Dunn et al. 2005). Finally, ATP can also activate microglia cells, satellite glia cells, immune cells and keratinocytes, which contribute to mechanisms of inflammatory and persistent pain (Julius and Basbaum 2001, Idzko, Ferrari et al. 2014).

As will be discussed in detail in Chapter 3, BomoTx induces intracellular calcium mobilization and ATP release from subpopulations of sensory neurons. This effect is not due to non-specific cell damage, but rather a signaling mechanism that involves pannexin channel opening, revealing a new endogenous nucleotide release pathway in sensory neurons. Moreover, this study has examined how BomoTx-evoked purinergic signaling contributes to nociception and pain, providing mechanistic insight into a major symptom associated with envenomations that are endemic to Latin America (Nishioka Sde and Silveira 1992, Campbell, Lamar et al. 2004).

Centipede venoms

Despite the diversity of venomous animals, most toxins characterized to date belong to a narrow taxonomical range (Undheim, Jones et al. 2014). Centipedes, which likely represent the oldest terrestrial venomous lineage next to scorpions (Undheim and King 2011), have received relatively little attention despite their importance as predatory venom-bearing arthropods (Undheim, Fry et al. 2015). Bites from centipedes produce

robust pain in humans (Balit, Harvey et al. 2004), as well as death in mammals (Undheim, Jones et al. 2014), indicating the existence of potential pain-producing toxins in their venoms. Identifying such toxins could provide new insights into pain mechanisms while also contributing to our knowledge of centipede venom composition and toxin evolution.

Recently, three studies (Liu, Zhang et al. 2012, Yang, Liu et al. 2012, Undheim, Jones et al. 2014) have described the composition and activities of toxins from several centipede species of different orders. From these studies, it is surprising to see that the protein-rich centipede venom contains toxins of diverse sizes and cysteine frameworks, which is in contrast to other arthropod venoms such as scorpions and spiders that are dominated by a single peptide fold (cysteine-stabilized $\alpha\beta$ fold, or CS$\alpha\beta$ fold, and inhibitor cysteine knot fold, or ICK fold, respectively) (Fry, Roelants et al. 2009, Undheim, Jenner et al. 2016). Consistent with the distinction from other arthropods, centipede venoms also seem to utilize different genetic strategies (such as multidomain transcripts) to generate mature toxins (Undheim, Sunagar et al. 2014).

There are high molecular weight enzymes found in centipede venoms, including serine proteases, metalloproteases and PLA$_2$s, which resemble those in the snake venoms (Undheim, Jones et al. 2014). More importantly, there are 24 phylogenetically distinct low molecular weight disulfide-rich peptide scaffolds, of which 19 are novel (Undheim, Jones et al. 2014, Undheim, Jenner et al. 2016). Only a few toxins have been

characterized in regard to their targets and function, including a helical arthropod-neuropeptide-derived (HAND) fold toxin μ-SLPTX-Ssm6a from *S. subspinipes mutilans* that inhibits $Na_v1.7$ (Yang, Xiao et al. 2013), RhTx that targets TRPV1 (Yang, Yang et al. 2015), and some others that target K_v and Ca_v channels (Liu, Zhang et al. 2012, Yang, Liu et al. 2012). Indeed, much still remains unknown in the centipede venom world.

Toxin cysteine frameworks for evolutionary analysis

Disulfide-rich peptide toxins are typically conserved in so far as the intramolecular disulfide frameworks that constrain their 3D fold and provide them with exceptional stability (King 2011). As a result, these cysteine frameworks are commonly used to group toxins into distinct structural classes (Rodriguez de la Vega and Possani 2004, Rodriguez de la Vega and Possani 2005, Undheim, Jones et al. 2014). While cysteines are highly conserved within toxins, most of the non-cysteine residues can be mutated without damaging the toxin's overall structural integrity (Sollod, Wilson et al. 2005, Undheim, Mobli et al. 2016), providing a mechanism for functional diversification. This high degree of molecular plasticity often leaves very few conserved residues for deep evolutionary analysis and thus, the cysteine framework and 3D fold remain the most important parameters for categorizing these rapidly evolving peptides as a means of recognizing distant evolutionary links (Undheim, Grimm et al. 2015). For example, the inhibitor cysteine knot (ICK) fold is one of the most widely conserved peptide folds found in arthropods, mollusks, sponges, plants and viruses (Undheim, Mobli et al. 2016).

Despite their sequence diversity, most of ICK toxins consist of the classical six-cysteine pattern with a similar 3D fold. Analysis of ICK folds from different organisms suggests that only one or two origin peptide species form the basis of the tremendous functional and structural diversity observed in nature (Parfrey, Lahr et al. 2011, Undheim, Mobli et al. 2016). Hence, utilizing toxin structural information can lead to more precise phylogenetic placement, which can suggest useful functional hypothesis and accurate evolutionary analysis.

In Chapter 4, I will describe the discovery of centipede toxins μ-SLPTX$_{15}$-Sm1a/b (henceforth Sm1a/b). They were initially identified based on their ability to activate subpopulations of sensory neurons. Sequence analysis and NMR structural studies have shown that this novel toxin disulfide framework contributes to a new type of CS$\alpha\beta$ fold, which resembles the 3D structure of scorpion defensin and K$^+$ channel blockers α-KTx (Miller 1995, Rodriguez de la Vega and Possani 2004, Luna-Ramirez, Bartok et al. 2014, Meng, Xie et al. 2016). This work provides insight into the functions of a previously unknown family of centipede toxins (Sm1a/b) and possibly their physiological effects on sensory neurons. In addition, these peptides may stand as an evolutionary link between centipede and scorpion toxins, providing insight into evolutionary origins of the CS$\alpha\beta$ fold (Sunagar, Undheim et al. 2013).

CHAPTER 2

Methods

Venom screen

Crude snake venoms were provided by the National Natural Toxins Research Center, Texas A&M University-Kingsville, Texas, USA. Crude centipede venoms were provided by Glenn King. Approximately 10mg of lyophilized crude snake venoms were dissolved in 200μl water and filtered through centrifugal filters with membrane molecular cutoff (MWCO) of 50kDa (Millipore). Filtered venoms were buffered in isotonic solution (140mM NaCl, 5mM KCl, 2mM $CaCl_2$, 2mM $MgCl_2$, 10mM glucose, 10mM HEPES, pH7.4) for ratiometric calcium imaging in sensory neurons. Neurons were previously loaded with Fura-2-AM (Molecular Probes) for >1 hour. Response to high extracellular potassium (150mM KCl, 10mM HEPES, pH7.4) was used to identify neurons. Venoms causing robust neuronal responses were kept for further analysis. All calcium imaging responses were digitized and analyzed using MetaFluor software (Molecular Device).

Toxin purification

In Chapter 3, crude *Bothrops moojeni* venom was dissolved in water to 100mg/ml, diluted 3-fold to 5% acetonitrile containing 0.1% trifluoroacetic acid (TFA), filtered through a 0.1-μm centrifugal filter unit (Millipore) and fractionated by reverse-phase HPLC. Up to 25mg venom was loaded onto a semi-preparative C18 column (Vydac model 218TP510), and eluted with a 19min linear gradient (15-70%; 3ml/min). Solvent A was 0.1% TFA in water and solvent B was 0.1% TFA in 90% acetonitrile. Fractions containing BomoTx was lyophilized, dissolved, diluted in 5% acetonitrile with 0.1% TFA, applied to an analytical C18 column (Vydac 218TP54) and separated with a 20-min

linear gradient (26-46%; 0.8ml/min). All purifications were performed at room temperature. Purified fractions were lyophilized, dissolved in water, aliquoted, and stored at -80°C. Protease (Sigma, P8811) digestion of the purified fraction was conducted in 37°C for up to 24hr and protease was heat inactivated at 85°C for 15min.

In Chapter 4, crude *Scolopendra morsitan* venom was fractionated on a Phenomenex 250x4.6mm i.d. Gemini C18 column (particle size 3μm, pore size 110Å), eluting venom components across a gradient of 5–50% solvent B (90% ACN, 0.43% TFA) in solvent A (0.5% TFA) at 1ml/min over 45 minutes. Components in active fraction were separated on a Phenomenex 100x3mm i.d. Onyx monolithic C18 column (pore size 130Å) across a gradient of 10–40% B at 3ml/min for 10 minutes.

Sequence determination

In Chapter 3, the freshly purified active fraction was mixed 1:1 (v/v) with Sinnapinic Acid (10mg/ml) then spotted onto the target. Data were collected over a range of 1,000-20,000 m/z on an Axima Performance MALDI-TOF/TOF mass spectrometer (Shimadzu) in linear mode and calibrated using the ProteoMass kit (Sigma). The molecular mass of the polypeptide was determined as 13,835Da. Only ions corresponding to this polypeptide were observed.

An aliquot of the fraction was diluted to feature a 20mM NH_4HCO_3 concentration, the disulfide bridges were reduced with DTT (30min, 60°C), and the free sulfhydryls were

alkylated with iodoacetamide (30min, room temperature). Tryptic digestion (2% (w/w) side-chain protected porcine trypsin, Promega) was performed at 37°C for 5hrs. The digest was analyzed by LC/MS/MS analysis using a Famos autosampler/Eksigent nanopump HPLC system directly linked to a QSTAR Elite (Sciex, Toronto, Canada) quadrupole-orthogonal-acceleration-time-of-flight mass spectrometer. The peptides were fractionated on a home made C18 column (100 μm ID x 150 mm) at a flow rate of 400μl/min. Solvent A was 0.1% formic acid in water and solvent B was 0.1% formic acid in acetonitrile. The sample was injected onto the column at 5% solvent B and a linear gradient was developed to 40% B over 35 min. Data acquisition was performed in an information-dependent manner: the two most abundant multiply charged ions were fragmented after each MS survey scan. The collision energy was automatically adjusted according to the precursors' m/z and z values. Dynamic exclusion was enabled.

From the raw data, a peaklist was generated using a Mascot script provided by the manufacturer. Protein Prospector (http://prospector.ucsf.edu/prospector/mshome.htm) was used for the database search, with the following parameters: enzyme = trypsin; carbamidomethylation of Cys = fixed modification; Acetylation of protein N-termini, Met oxidation, and cyclization of N-terminal Gln residues = variable modifications; mass error permitted = 200 and 300 ppm for precursor ions and fragments, respectively. First we searched the SwissProt.2012.03.21 database, without species specification (535248/535248 entries searched), permitting only 1 missed cleavage in order to ascertain that there were no unexpected protein contaminations in the sample, then a

species specific (*Bothrops moojeni*) search was performed using the NCBInr.2011.01.09 database (27/12679686 entries searched), with 3 missed cleavages permitted in order to achieve the best possible sequence coverage.

The sequences identified unambiguously indicated that the active ingredient must be a new phospholipase. Homology considerations (to NCBI entries 17865560 and 17368325, and UniProt entry Q9PVE3) and manual *de novo* sequencing led to a tentative full sequence determination:

SLVELGKMILQETGKNPVTSYGAYGCNCGVLGRGKPKDATDRCCYVHKCCYKKLTDCNPKKDRY

SYSWKDKTIVCGENNSCLKELCECDKAVAICLRENLDTYNKKYKNNYLKPFCKKADPC

The sequence was confirmed by translating the open reading frame. The calculated MW = 13,834 (with all Cys residues in disulfide bridges) shows good agreement with the experimentally determined value. The sequence information can be found in NCBI GenBank with accession number KX856005.

When determining the protease (Sigma, P8811) digestion results, standards were mixed with the sample including Angiotensin II (Sigma A8846), ACTH fragment 18-39 (Sigma A8346), Insulin oxidized B chain (Sigma I6154), Insulin (Sigma I6279), Cytochromme c (Sigma C8857) and Apomyoglobin (Sigma A8971).

In Chapter 4, fractions were digested, analyzed and searched against transcriptome as previously described (Undheim, Sunagar et al. 2014). Briefly, fractions were spotted directly onto a MALDI plate using a Shimadzu Accuspot NSM-1 before batch analysis

using a 4700 MALDI TOF/TOF Proteomics Analyser (AB Sciex) in positive reflectron mode; ions of m/z 900–8000 were acquired by accumulating 2500 laser desorptions/spectrum. Samples were analyzed twice, using either α-cyano-4-hydroxycinnamic acid (CHCA) or 1,5-diaminonaphthalene (1,5-DAN) as matrix. For CHCA-spotted samples, high intensity ions with m/z <3500 were manually selected for MS/MS. MS/MS experiments were run twice, with and without nitrogen gas in the collision cell for collision induced dissociation (CID), in both cases using a relative mass precursor window of 200 resolution (full width at half maximum), enabling metastable ion suppression, and accumulating 2000 shots/spectrum.

Correct sequence and post-translational modifications were checked by MALDI-TOF/TOF, MALDI-ISD-TOF/TOF-MS. For generation of sequence tags by in-source decay (ISD) using 1,5-DAN, sample spots corresponding to >95% pure peptide larger than 3kDa (as determined from initial analysis using CHCA) were re-spotted using 1,5 DAN matrix and immediately analyzed using ISD. Mass ranges were set from m/z 1000 up to 200 m/z higher than the precursor ion; up to 10 acquisition rounds were accumulated to maximize resolution and signal-to-noise ratio (S/N) for fragment ions. ISD spectra were manually interpreted, while CID spectra were automatically searched against the respective transcriptomes translated to all reading frames using Protein Pilot v4.5 (AB Sciex). The searches allowed for biological modifications and amino acid substitutions. Spectra were inspected manually to eliminate false positives, excluding spectra with low S/N, erroneous modification assignments, and confidence values below

99%.

BomoTx cDNA cloning

Deduced sequences covering the mature BomoTx were used to clone full-length BomoTx cDNAs. RNA was extracted from one *Bothrops moojeni* venom glands using TRIZOL reagent (Invitrogen), then isolated by chloroform extraction and isopropanol precipitation. A cDNA library was generated for use in 5' and 3' rapid amplification of cDNA ends (RACE) reactions using SMARTer RACE cDNA Amplification Kit (Clontech). Degenerative primers were designed to amplify fragments of BomoTx sequences covering the 5' and 3' UTR, which were sequenced after insertion into TOPO vector (Invitrogen). The 5' and 3' UTR sequences were used to design specific primers to amplify the full-length cDNA. The cDNA-derived peptide sequence agreed with observed molecular mass of the purified toxins, assuming the presence of disulfide bridges. $sPLA_2$ activity was assessed using $sPLA_2$ Assay Kit (Cayman Chemical).

Sm1a synthesis

The primary structure of Sm1a was synthesized using Fmoc chemistry, and disulfide bond formation was initially achieved with random oxidation using NH_4HCO_3. The three resulting disulfide isomers of Sm1a were purified using RP-HPLC. The native isomer was identified with two pieces of evidence. Firstly, naturally isolated Sm1a co-eluted with one specific isomer. Secondly, only that isomer gave good amide proton resonance dispersion in NMR spectra, which indicates it is the only isomer to adopt a well-defined

tertiary structure. The disulfide connectivity was determined using enzymatic digests and synthesis. Briefly, GluC digest of naturally isolated Sm1a disqualified the I-II, III-IV connectivity as being native. The remaining two possible isomers (I-III, II-IV and I-IV, II, III) were then both synthesized using a directed Acm protecting group approach to see which isomer had the same retention time and NMR spectra as the native isomer. This data revealed that the I-III, II-IV isomer is the native disulfide connectivity of Sm1a.

Sm1a NMR

NMR samples were prepared by dissolving Sm1a (1mg) in a 90% H_2O/ 10% D_2O mixture (500μL) containing 20mM NaPi (pH ~5.9). NMR measurements were recorded on a Bruker Avance 600MHz spectrometer at 298K. 2-D TOCSY, NOESY, E-COSY, and natural abundance 15N and 13C HSQC were used to sequentially assign backbone and side chain protons. Variable temperature experiments were performed by recording six TOCSY spectra at temperatures ranging from 283 – 308K. Slowly exchanging amide protons were identified by incubating Sm1a in pure D_2O over 24 hours. Solvent suppression was achieved using excitation sculpting. Spectra were referenced to water at 4.77ppm. All Spectra were processed using Topspin 2.1 and assigned using CcpNMR Analysis (Vranken, Boucher et al. 2005).

Initial structure calculations were performed using the program CYANA with distance restraints derived from NOESY spectra. Disulfide restraints were introduced along with backbone φ and ψ dihedral angle constraints generated using TALOS-N (Shen and Bax

21

2013). X1 restraints were derived from E-COSY coupling constants and NOE intensities. Hydrogen bond restraints were introduced as indicated by slow D2O exchange and for those backbone amide protons whose chemical shift was not temperature sensitive. A final set of structures was refined by CNS (Brunger 2007) using torsion angle dynamics, refinement and energy minimization in explicit solvent, and protocols as developed for the RECOORD database (Nederveen, Doreleijers et al. 2005). A final set of 20 lowest energy structures was chosen based upon stereochemical quality as assessed using MolProbity (Chen, Arendall et al. 2010).

Sensory neuron culture

Trigeminal ganglia were dissected from newborn (P0–P3) C57BL/6 mice or rat and cultured for >12 hours before calcium imaging or electrophysiological recording. Primary cells were plated onto cover slips coated with poly-L-lysine (Sigma) and laminin (Invitrogen, 10µg/ml). Embryonic DRG cultures were generously provided by Jonah Chan (Lewallen, Shen et al. 2011). Embryonic cultures were maintained as described and transduced with freshly made lentivirus supernatant at DIV4. Calcium imaging experiments were performed at DIV14.

Lentivirus Production

HEK293T cells were maintained in DMEH-21 medium with 10% fetal bovine serum (FBS) and penicillin streptomycin in 5% CO_2 at 37°C. Lentivirus was produced by transfecting HEK293T cells with FUGW-rat $P2X_2$, psPAX2 and pVSVG using Fugene

HD (Roche) according to the manufacturer's instructions.

Electrophysiology

TG neuron whole-cell recording extracellular solution contained 150mM NaCl, 2.8mM KCl, 1mM $MgSO_4$, 2mM $CaCl_2$, 10mM HEPES, 290-300mOsmol/kg, pH7.4. Pipette solution contained 130mM K-gluconate, 15mM KCl, 4mM NaCl, 0.5mM $CaCl_2$, 1mM EGTA, 10mM HEPES, 280-290mOsmol/kg, pH7.2. For whole-cell recordings from HEK293 cells, the extracellular solution contained 150mM NaCl, 2.8mM KCl, 1mM $MgSO_4$, 2mM $CaCl_2$, 10mM HEPES, 290-300mOsmol/kg, pH7.4. Pipette solution contained 130mM CsMeSO3, 15mM CsCl, 4mM NaCl, 5mM BAPTA, 10mM HEPES, 280-290mOsmol/kg, pH7.4. Whole-cell patch clamp of cultured mouse TG neurons and HEK293 was performed as described (Bohlen, Priel et al. 2010). Extracellular solution was perfused with or without toxins/drugs using a SmartSquirt Micro-Perfusion system (AutoMate). All recordings were performed using fire-polished glass electrodes with a resistance of 2–5MΩ at room temperature (20–22°C). Signals were amplified using an Axopatch 200B amplifier, digitized with a Digidata 1440A and recorded using pCLAMP 10.2 software (Molecular Devices, Sunnyvale, CA, USA). For all DRG neurons the holding potential was –80mV. Drugs used in the work: capsaicin (10nM, Sigma), menthol (100µM, Sigma), AITC (100µM, Sigma), TTX (500nM, Tocris), lidocaine (1mM, Tocris), ruthenium red (10µM, Sigma), apyrase (2-20U, Sigma), Ro51 (100nM, Tocris), ATP (50µM, Sigma), α,β-MeATP (50µM, Sigma), carbonoxolone (10µM, Sigma), niflumic acid (100µM, Tocris), flufenamic acid (100µM, Tocris), monensin (100µM,

23

Tocris), N-ethylmaleimide (100µM, Sigma), YO-PRO-1Iodide (500nM, Thermo Fisher Scientific), thapsigargin (2µM, Tocris), U73122 (10µM, Sigma), Z-VAD-FMK (100µM, Tocris), Evans blue dye (30mg/kg, Sigma).

Behavior

Mice were bred and housed in accordance with UCSF Institutional Animal Care Committee (IACUC) guidelines. 2–5 animals were housed together on a 12-h light/dark schedule with constant access to food and water. Behavioral experiments were approved by UCSF IACUC and were in accordance with the National Institutes of Health (NIH) Guide of the Care and Use of Laboratory Animals and the recommendation of the International Association for the Study of Pain. P2X$_2$/P2X$_3$$^{dbl-/-}$ mice were generously provided by Dr. Thomas E Finger (Department of Cell and Developmental Biology, University of Colorado School of Medicine). Intraplantar injections (20µl PBS+0.1% BSA, with or without 50µM BomoTx) were performed on adult (10- to 18-week-old) mice. Nocifensive responses were recorded during a 20min observation period immediately following intraplantar injections. Licking and lifting behavior was scored with the experimenter blinded to injection condition and experimental cohort. Hargreaves and Von Frey tests were performed 15 min after intraplantar injection of 5µM BomoTx to measure heat and mechanical sensitivity, respectively. Intrathecal (i.t.) capsaicin ablation was performed as previously described (Cavanaugh, Lee et al. 2009) and ablation was confirmed by hot plate test and histology. Evans Blue dye (30mg/kg) was administered retro-orbital into the mice retrobulbar sinus 1 min before intraplantar

application of BomoTx (50µM and 5µM) or capsaicin (5µM). Mice were euthanized 30min after application of the stimulus. The skin of the hindpaws was removed and the extravasated dye extracted in formamide for 48 h at 65°C in the dark and measured by using a spectrophotometer (620nm). For ATF3 staining, mice hindpaws were injected with 20µl PBS+0.1% BSA with 50µM BomoTx, 5% formalin or 30µM α,β-MeATP. Mice were euthanized 2 days after the injection. Male and female mice were first considered separately in hindpaw nocifensive response experiments. Both sexes showed significantly greater responses to toxin than vehicle control. Therefore, male and female behavioral responses were pooled and subsequent experiments were performed on both male and female mice.

Immunohistochemistry

Mice were deeply anesthetized with pentobarbital then transcardially perfused with 10ml of phosphate buffered saline (PBS) followed by 10ml of 10% neutral buffered formalin (NBF). Spinal cord lumbar sections or DRGs were dissected, post-fixed in 10% NBF at room temperature for 2 hours, cryoprotected in PBS with 30% w/v sucrose overnight at 4°C, then embedded in OCT Compound at –20°C. Tissue was sectioned at 25µm, thaw-captured on Diamond White Glass slides (Globe Scientific), and stored at –20°C until use. Slides were incubated for 1h at RT in a blocking solution consisting of PBS with 0.2% v/v Triton X-100 (Sigma), 0.1% BSA and 2% normal goat serum (NGS). Slides were then incubated in primary antibody overnight at 4°C, then washed in fresh PBS 3X, incubated in secondary antibody for 1 h at RT in the dark. Sections were then washed in

fresh PBS 3X prior to mounting with ProLong Gold antifade reagent with DAPI (Life Technologies) and coverslipping. Images were acquired with a Leica DMRB microscope and DFC500 digital camera using Leica Application Suite v3.5.0 then further analyzed using ImageJ software. We used fluorophore-conjugated secondary antibodies raised in goat against rabbit (1:1000, Alexa Fluor 488, Life Technologies). Fos staining was performed 60 min after hindpaw injection of BomoTx or PBS. Rabbit anti-Fos (CalBiochem) was used 1:30000, followed by biotinylated goat anti-rabbit antibody (Vector Labs, Burlingame, CA, 1:200), avidin–biotin conjugate, and nickel-enhanced diaminobenzidine detection (Vectastain ABC, Vector Labs). ATF3 antibody (Santa Cruz Biotechnology) was used at 1:2000.

Cell death assay

Primary sensory neurons or HEK293 cells were seeded at 50μl 30,000 cells/well in white opaque 96-well plates and incubated overnight at 37°C in 5% CO_2. BomoTx were diluted with buffer (140mM NaCl, 5mM KCl, 2mM $CaCl_2$, 2mM $MgCl_2$, 10mM glucose, 10mM HEPES, pH7.4) and delivered to cells for 5min before luminogenic cell-impermeant peptide substrate (AAF-aminoluciferin) from CytoTox-Glo^{TM} (Promega) is added to measure dead-cell protease activity. Lysis reagent was added at the end to induce cell death in to reveal total cells, as described in manufacture's instructions.

Statistics

Data were analyzed using Prism 6 software (GraphPad Software, San Diego, CA, USA)

and significance testing used one-way analysis of variance (ANOVA), followed by post hoc Tukey's test, as noted in Figure legends. All significance tests are two-sided. Significance levels are $*p < 0.05$, $**p < 0.01$, $***p < 0.001$, and $****p < 0.0001$. The number of experiments (n) and significance are reported in the Figure legends. Sample sizes for cellular physiology, histology and animal behavior were chosen based on previous experience with these assays as the minimum number of independent observation required for statistically significant results. We assume equal variance and normally distributed data within experimental paradigms where comparisons are made. These are common assumptions relied upon for significance testing within these experimental paradigms as previously published by our group and others.

CHAPTER 3

A Novel Brazilian Lancehead Pit Viper Toxin Elicits Pain

Through Regulated ATP Release

Introduction

Venoms from spiders, snakes, cone snails and scorpions have evolved to produce a vast pharmacopoeia of toxins that modulate receptor or channel function as a means of producing shock, hemolysis, paralysis and pain (Julius and Basbaum 2001, Fry, Roelants et al. 2009). As such, venoms from these animals represent a rich potential source of potent and selective toxins that can be exploited to study and manipulate somatosensory and nociceptive signaling pathways. For example, toxins can directly target ion channels expressed by nociceptive sensory neurons to elicit or inhibit pain. Well-validated examples include toxins that target TRP, ASIC, and Na_v channels (Bohlen, Priel et al. 2010, Bohlen, Chesler et al. 2011, Diochot, Baron et al. 2012, Cao, Liao et al. 2013, Baconguis, Bohlen et al. 2014, Osteen, Herzig et al. 2016). However, the 'toxinome' is incredibly diverse and there are many pain-producing venoms for which the responsible toxins have not yet been identified.

In addition to targeting receptors and channels directly, algogenic toxins could also promote the synthesis and/or release of metabolites, transmitters, or second messengers that activate primary afferent nociceptors. While this could occur through indiscriminate actions of venom lipases and proteases that release cellular contents through tissue damage and cell death, more specific mechanisms may also exist. Their identification could reveal important new pathways by which exogenous or endogenous pain-producing agents mediate their effects.

To identify novel pain-producing toxins, we have exploited cultured sensory neurons as a facile *in vitro* platform for unbiased screening of crude venoms, optimizing conditions to reduce non-specific cell damage so as to reveal toxins having specific cellular effects. With this approach, we have identified a novel toxin (BomoTx) from the Brazilian lancehead pit viper (*Bothrops moojeni*) found mainly in Brazil. BomoTx belongs to a group of secreted phospholipase A2 (sPLA2)-like proteins that have the conserved PLA2-fold but lack enzymatic activity and is most closely related to so-called 'Lys49 myotoxins' found in snake species within the *Crotalinae* subfamily (Gutierrez and Lomonte 2013). These toxins are devoid of phospholipase activity due to key enzymatic site mutation of Asp49 to Lys49, but promote release of ATP from myotubes through an as-yet uncharacterized mechanism (Montecucco, Gutierrez et al. 2008, Cintra-Francischinelli, Caccin et al. 2010, Fernandes, Borges et al. 2014). Similarly, we show that BomoTx lacks phospholipase activity and excites a cohort of sensory neurons through a mechanism involving ATP release and activation of $P2X_2$ and $P2X_3$ purinergic receptors. Furthermore, we provide pharmacological and electrophysiological evidence to support a role for pannexin hemichannels in mediating toxin-evoked nucleotide release. At the behavioral level, injection of BomoTx into the mouse hind paw elicits non-neurogenic inflammatory pain, thermal hyperalgesia and mechanical allodynia. The latter is completely dependent on purinergic signaling. Together, these findings elucidate a detailed mechanism by which a Lys49 myotoxin produces pain associated with envenomations common to Latin America (Campbell, Lamar et al. 2004).

Results

A novel snake toxin that targets somatosensory neurons

To identify novel toxins that target nociceptors, we used live-cell calcium imaging to screen a library of 22 snake venoms for their ability to activate primary sensory neurons cultured from rat trigeminal ganglia (TG). Because many snake venoms contain cytolytic components, such as proteases and lipases (Fry, Roelants et al. 2009, Casewell, Wuster et al. 2013), initial screening of these samples resulted in cell injury and widespread calcium influx that masked the action of any specific components. To circumvent this problem, we first processed all crude venoms through a 50 kD molecular weight cutoff filter to enrich for peptides and small proteins. Indeed, this eliminated background activities in more than half of the crude venoms examined. Among these, filtrates from *Bothrops moojeni* (Brazilian lancehead) (Figure. 1A) robustly activated a subpopulation of TG neurons (Figure. 1B). Fractionation of this crude venom by reversed phase (C_{18}) chromatography yielded a single active peak (Figure. 5A), that recapitulated activity observed with the crude venom.

To determine the toxin's identity, we analyzed purified toxin by MALDI-TOF mass spectrometry (MS), revealing a single polypeptide with a molecular mass of 13,835 Da (Figure. 5C). The sample was then trypsin digested and analyzed by liquid chromatography-tandem mass spectrometry (LC/MS/MS). Homology considerations (to NCBI entries 17865560 and 17368325, and UniProt entry Q9PVE3) and manual *de novo* sequencing provided tentative full sequence determination, which was then used to clone the full-length (122 amino acid) complementary DNA (cDNA) from the Brazilian

lancehead venom gland. Indeed, the amino acid sequence translated from the toxin's open reading frame was identical with the proposed sequence, and the molecular mass calculated from it matched the experimentally determined results, assuming the presence of disulfide bridges. This species, which we call BomoTx, is a novel PLA2-like toxin whose pattern of cysteine residues classifies it specifically within a group known as Lys49 myotoxins (Figure. 5H) (Gutierrez and Lomonte 2013). Like other members of this myotoxin family, BomoTx has a lysine in place of a critical aspartate residue within the latent enzymatic pocket, and thus has retained the compact and stable fold of a PLA2-like protein, but is devoid of catalytic activity (Figure. 5B).

BomoTx elicited two types of responses in neurons: large, sustained calcium signals in one group of TG neurons (Figure. 1C), and small, transient signals in a separate subpopulation (Figure. 1D). In addition, we also observed some calcium responses in fibroblasts, the majority of which were in the vicinity of neurons that exhibited sustained calcium signals (Figure. 1E, 6B). These responses were evoked by BomoTx alone, as digested BomoTx no longer activated any neurons (Figure. 5D-G). Since BomoTx closely resembles Lys49 myotoxins (Figure. 5H), which are reported to cause ATP release from muscle cells (Cintra-Francischinelli, Caccin et al. 2010), we wondered if ATP signaling is involved in the responses we observed. Co-application of ATP diphosphohydrolase apyrase eliminated transient toxin-evoked responses in both neurons and fibroblasts (Figure. 1G, H), but not sustained responses in neurons

(Figure. 1F). We conclude that ATP release is, indeed, required for transient toxin-evoked responses.

To more fully categorize these BomoTx-sensitive populations, we examined overlap between toxin-evoked responses and other functional or histological markers (Figure. 6A). Of the transient responders (Figure. 1J), most responded to ATP and α,β-MeATP (87.0±12.1%, 93.8±8.8%, respectively), which activate homomeric and heteromeric P2X$_3$ and P2X$_{2/3}$ purinergic receptors. A substantial percentage of transient responders also responded to agonists for TRPV1, TRPA1, TRPM8 and/or Nav1.1 channels, and most (72.0±18.9%) bound the lectin, IB4. Taken together, these results indicate that these small to medium diameter transiently responding population of BomoTx-sensitive neurons consists of both non-peptidergic C fibers as well as peptidergic Aδ fibers. In contrast, neurons showing sustained toxin responses exhibited minimal overlap with TRPV1 (17.6%) or TRPA1 (0%) agonists, and relatively few responded to ATP (27.3%) or α,β-MeATP (0%) (Figure. 1I). These sustained responders were also of larger diameter (Figure. 1K), suggesting that they correspond to non-nociceptive Aα/Aβ neurons.

BomoTx-evoked transient responses are mediated by purinergic signaling

To address the basis of the toxin sensitivity in transiently responding neurons, we carried out whole-cell patch-clamp analysis of cultured TG neurons, which revealed a toxin-evoked inwardly rectifying current (Figure. 2A). Consistent with our

33

pharmacological profiling by calcium imaging, extracellular ATP could invariably elicit currents in these neurons (Figure. 2B). Moreover, Ro51, a specific blocker of $P2X_3$ and $P2X_{2/3}$ ionotropic subtypes (Jahangir, Alam et al. 2009), reduced toxin-evoked responses by 72.2±5.3% (Figure. 2B).

Does BomoTx elicit its response by activating P2X receptors directly, or by promoting release of ATP? To address this question, we first asked whether the toxin elicits membrane currents in transfected HEK293 cells expressing $P2X_2$ and/or $P2X_3$ receptors. No responses were observed (Figure. 2C), nor did the toxin shift dose-response curves for ATP (Figure. 7A), indicating that BomoTx is not a direct purinergic receptor agonist or modulator. Hence, the toxin likely promotes release of ATP to activate transient responses in specific sensory neurons that express purinergic receptors.

If ATP-evoked activation of P2X receptors accounts for BomoTx sensitivity in transiently responding neurons, ectopic expression of these channels in sensory neurons should increase the prevalence of toxin responsive cells. We therefore transduced embryonic rat dorsal root ganglia (DRG) neurons with lentivirus carrying the full-length rat $P2X_2$ cDNA. After seven days of expression, >95% of neurons responded to ATP or α,β-MeATP, compared to <20% in vector-infected or uninfected control cultures (Figure. 2D), demonstrating efficient ectopic expression of P2X receptors. Under these circumstances, BomoTx sensitivity was also more prevalent (20.12%) compared to

controls (2.98%). Interestingly, activated neurons tended to cluster, supporting a possible ATP release and signaling mechanism. Furthermore, application of apyrase attenuated these transient BomoTx-evoked responses to 1.71% (Figure. 2D, 7B), but not sustained responses. Together, these results support the notion that BomoTx excites a subpopulation of sensory neurons by promoting release of ATP, followed by activation of $P2X_2$ and/or $P2X_3$ receptors.

BomoTx-induced ATP release requires hemichannels

In the lentiviral transduced embryonic DRG cultures, >99% of the cells are post-mitotic neurons (Figure. 8A) and thus extracellular ATP could be released from neurons. As BomoTx produces a sustained calcium response within a subpopulation of neurons that do not show sensitivity to apyrase, we hypothesized that these neurons might be the source of ATP release.

As noted above, BomoTx lacks PLA2 enzymatic activity and thus loss of membrane integrity through lipase action is unlikely to be the cause of ATP release. Moreover, BomoTx was cytotoxic only at relatively high concentrations (Figure. 7D) far exceeding that required for repetitive transient responses. BomoTx also demonstrated specificity towards neurons and myotubes as it failed to elicit calcium responses in a variety of other cell types, including glia-derived cell lines, smooth muscle cells, myeloblast-derived cell lines and HEK293 cells (Figure. 7E). Taken together, these findings suggest that ATP released is not due to non-specific cell damage or death.

In considering more specific mechanisms of toxin-evoked ATP release, we asked whether this could involve hemichannels or neuronal vesicles, which represent two main candidates for mediating non-lytic mechanisms of nucleotide release (Dahl 2015). First, we tested effects of the vesicle release inhibitors, N-ethylmaleimide (NEM) and monensin, neither of which affected BomoTx-evoked responses (Figure. 8B). In addition, DRG neurons transduced with lentivirus carrying the long chain of tetanus toxin did not show reduced toxin sensitivity. Thus, a vesicular mechanism does not seem to underlie toxin-evoked ATP release.

We next asked whether blockers of pannexin and connexin hemichannels, such as carbenoxolone (CBX), niflumic acid (NFA), or flufenamic acid (FFA), could attenuate toxin sensitivity. Indeed, all of these agents dose-dependently reduced the number of BomoTx-sensitive neurons (Figure. 8C, D); furthermore, blockade at low CBX concentrations is indicative of a role for pannexin channels. Consistent with this, low concentrations of CBX also blocked ATP release in P0 TG cultures (Figure. 3A). Taken together, we conclude that BomoTx elicits neuronal ATP release through a hemichannel-mediated pathway, likely involving pannexins.

We then investigated if BomoTx-induced pannexin opening underlies sustained toxin responses. Pannexins pass large molecules such as the dye, YO-PRO-1, enabling us to ask whether pannexin opening correlates with sustained toxin-evoked calcium

36

responses. In fact, we observed 93% overlap of these responses (Figure. 3B). Importantly, CBX-sensitive currents were also detected in these neurons, but not those exhibiting transient activation by BomoTx (Figure. 3C). Furthermore, pannexin itself is not sensitive to BomoTx, as HEK293 cells expressing Pannexin 1, with or without Pannexin 2, show no response to BomoTx (Figure. 8E, F). These results suggest that BomoTx indirectly elicits pannexin opening and release of ATP, thus activating $P2X_2/X_3$ receptors and giving rise to transiently responding sensory neurons. Consistent with this mechanism, cells with YO-PRO-1 uptake (indicating a sustained toxin-evoked population) (Figure. 3D, I) demonstrated intracellular calcium release caused by BomoTx. These responses could induce various magnitudes of store-operated calcium entry (SOCE) (Figure. 3D), and were attenuated by pre-treatment with thapsigargin and U73122 (Figure. 3F, G), suggesting that BomoTx promotes release of calcium from intracellular stores via PLC pathways in these cells. On the other hand, toxin-evoked apyrase-sensitive transient responses depended on extracellular calcium, and were not accompanied by YO-PRO-1 uptake (Figure. 3D, E, H, I).

Thus, we conclude that (Figure. 3J) BomoTx evokes intracellular calcium release from a specific population of sensory neurons. Subsequent signaling events lead to hemichannel pannexin opening to release ATP to the extracellular environment. Released ATP then activates purinergic signaling in sensory neurons through $P2X_2$ and/or $P2X_3$, which are the major purinergic receptors on these cells. Because pharmacologic blockade of these channels does not eliminate all transient responses,

other P2X and/or P2Y receptors likely contribute to residual toxin sensitivity in some neural and non-neural cells (Lewis, Neidhart et al. 1995).

BomoTx evokes pain and produces thermal and mechanical sensitization

Because BomoTx excites presumptive nociceptors, we asked whether it produces pain-like behaviors when injected into the mouse hindpaw. Indeed, nocifensive reponses were observed (Figure. 4A), including robust licking of the injected paw that was accompanied by edema (Figure. 9A). Abundant Fos expression was induced in superficial laminae of the ipsilateral dorsal spinal cord (Figure. 4B, C), consistent with activation of nociceptive pathways. In contrast, BomoTx did not induce expression of ATF-3, a marker of nerve damage, in lumbar DRG neurons (Figure. 9E), consistent with our cellular data suggesting that toxin-evoked responses are not simply a consequence of neuronal death.

We next asked if BomoTx promotes persistent pain. We injected toxin into the hindpaw at a dose insufficient to generate acute pain, and after 30 minutes assessed sensitivity to thermal or mechanical stimuli. We observed significant hypersensitivity to heat as evidenced by decreased paw withdraw latency in the Hargreaves assay (Figure. 4D), as well as mechanical hypersensitivity as measured by decreased paw withdraw threshold in the von Frey assay (Figure. 4E).

BomoTx-induced pain and sensitization were accompanied by paw edema, and we therefore asked whether TRPV1-positive neurons, which play a key role in heat hypersensitivity and neurogenic inflammation, contribute to toxin-evoked nocifensive behaviors. In animals in which the central projections of TRPV1-positive fibers were ablated by spinal (intrathecal) capsaicin injection (Figure. 9B, C), BomoTx-evoked acute pain was significantly reduced (Figure. 4A), as was Fos expression in the spinal cord (Figure. 4B, C). These animals also showed complete loss of toxin-induced heat hypersensitivity (Figure. 4D). In contrast, BomoTx-evoked mechanical hypersensitivity was unaffected (Figure. 9D), consistent with the fact that TRPV1–expressing fibers are essential for thermal, but not mechanical hypersensitivity (Cavanaugh, Lee et al. 2009, Mishra and Hoon 2010).

Because ATP-evoked $P2X_2/X_3$ responses (i.e. transiently responding neurons) constitute a major component of BomoTx signaling, we asked whether $P2X_2/X_3$ activation also contributes to the observed behavioral responses. We compared toxin-evoked nocifensive behaviors, as well as heat and mechanical sensitization in both WT and $P2X_2/P2X_3^{dbl-/-}$ mice (Cockayne, Hamilton et al. 2000, Cockayne, Dunn et al. 2005). Strikingly, elimination of $P2X_2$ and $P2X_3$ significantly attenuated mechanical sensitization (Figure. 4E) without diminishing acute nocifensive behaviors (Figure. 4A) or thermal sensitization (Figure. 4D). When $P2X_2/P2X_3^{dbl-/-}$ mice were treated with intrathecal capsaicin, acute toxin-evoked nocifensive behavior was completely lost

(Figure. 4A), demonstrating that TRPV1- and $P2X_2/P2X_3$-expressing fibers together account for all toxin-evoked acute behaviors.

BomoTx promotes non-neurogenic inflammation

BomoTx causes ATP release from neurons, which can target many other cell types in the nerve terminals, such as keratinocyte, macrophage and immune cells (Idzko, Ferrari et al. 2014). We therefore asked if toxin-induced inflammation and paw edema are neurogenic (i.e. require initial activation of substance P-expressing sensory nerve fibers). We measured toxin-evoked paw edema and Evan's blue dye (EBD) uptake in preprotachykinin A-deficient mice ($PPTA^{-/-}$), which do not exhibit neurogenic inflammation (Cao, Mantyh et al. 1998). As expected, these animals show minimal paw edema and EBD uptake after capsaicin injection (Figure. 4F, 9F, 9G). However, in both WT and $PPTA^{-/-}$ mice, BomoTx induced robust paw swelling and EBD uptake in the ipsilateral paws, at both high and low toxin doses (Figure. 4F, 9F, 9G).

Taken together (Figure. 4G), these observations suggest that BomoTx produces swelling and edema through a non-neurogenic mechanism involving ATP action on immune or other non-neural cell types in the local tissue environment. ATP and other inflammatory agents act on TRPV1-positive neurons to elicit acute pain behaviors(Bland-Ward and Humphrey 1997) and heat hypersensitivity. Furthermore, ATP signaling through $P2X_2$ and $P2X_3$ receptors on TRPV1-negative sensory neurons contributes to toxin-evoked mechanical sensitization, consistent with the fact that non-

TRPV1 Aδ fibers, which also express $P2X_2$ and $P2X_3$, are involved in mechanical hypersensitivity (Tsuda, Koizumi et al. 2000, Osteen, Herzig et al. 2016).

Discussion

We have identified a pain-inducing Lys49 myotoxin, BomoTx, which activates the pannexin pathway and two groups of sensory neurons. These groups include (i) a transiently responding cohort representing non-peptidergic C and Aδ fibers whose activation depends on P2X receptors and (ii) a cohort in which toxin-evoked sustained responses require intracellular calcium signaling and involve activation of pannexin hemichannels. We propose that BomoTx elicits nucleotide release from neurons showing sustained responses through hemichannel activation, thereby promoting activation of P2X receptors on transiently responding neighbors. We also observed BomoTx-evoked nocifensive behaviors, including acute pain accompanied by non-neurogenic inflammation, as well as thermal hypersensitivity – both mediated mainly through TRPV1-positive fibers. Furthermore, the toxin produced mechanical allodynia that required purinergic signaling through non-TRPV1, $P2X_2$ and/or $P2X_3$-positive neurons, likely representing Aδ fibers. Together, these findings support a role for regulated release of endogenous nucleotides in nociception, as well as involvement of ionotropic P2X receptors in mechanical hypersensitivity.

BomoTx relationship to Lys49 myotoxins

Lys49 myotoxins are a family of proteins that displays myotoxicity despite being catalytically inactive. BomoTx contains key protein sequence features of Lys49 myotoxins and it also activates C2C12 myotubes (but not C2C12 myoblasts), thereby a true member of the family of Lys49 myotoxins. It has been reported that ATP release contributes to the Lys49 myotoxin-induced myotoxicity, but detailed mechanisms remain unknown and it is unclear how toxin specificity toward myotubes (but not myoblasts and other cells types) is achieved. It has been hypothesized that Lys49 myotoxins interaction with membrane receptors that determine their specificity of action, but to-date no such receptors have been identified. Here we describe a potential pathway underlying BomoTx action that involves intracellular calcium signaling and pannexin hemichannel activation, providing evidence that ATP release by this family of snake toxins occurs through a specific cellular signaling pathway, rather than indiscriminate cellular injury. Moreover, we show that BomoTx induces Ca^{2+} responses in a subset of sensory and hippocampal neurons, as well as myotubes, but not other cell types tested, and the time course of ATP release is much faster (within 1min) than that reported for other membrane damaging toxins (5-20min) (Belmonte, Cescatti et al. 1987, Skals, Jorgensen et al. 2009). Hence, at lower concentrations, BomoTx exerts biological functions specific to neurons (or muscles) that do not require membrane disruption. It is possible that this specificity is achieved by the presence of different signaling components (receptors, calcium release mechanisms, pannexin). Still, as in the case of

Lys49 myotoxins, the exact mechanism underlying cellular specificity and/or the existence of a *bona fide* BomoTx receptor remains unknown.

Involvement of hemichannels in toxin-evoked ATP release

Pannexin1 can be activated by several stimuli including caspase activation (Chekeni, Elliott et al. 2010), Rho signaling (Seminario-Vidal, Okada et al. 2011), and mechanical stretch (Bao, Locovei et al. 2004). Here we observed BomoTx-evoked intracellular Ca^{2+} release via the PLC pathway and YO-PRO-1 uptake in cells that also display CBX-sensitive pannexin currents. Hence, we suggest that BomoTx-induced intracellular Ca^{2+} elevation occurs upstream of pannexin activation. However, since neurons exhibiting transient toxin-evoked or ATP evoked Ca^{2+} influx do not develop pannexin currents, consistent with previous observations (Seminario-Vidal, Okada et al. 2011), increased cytoplasmic Ca^{2+} per se may not be sufficient to activate pannexin currents. As such, we hypothesize that additional signaling steps are required to connect BomoTx-induced Ca^{2+} increases to pannexin activation.

Distinct fibers types contribute to BomoTx-evoked acute and persistent pain

Bothrops species are responsible for the majority of snake-related deaths and injuries in Latin America. Pain and tissue inflammation are hallmarks of viperid snake bites; other common symptoms include blisters, necrosis and hemorrhage (Nishioka Sde and Silveira 1992, Nishioka, Silveira et al. 2000, Campbell, Lamar et al. 2004). *Bothrops moojeni* venom contains a complex mixture of metalloproteinases (Bernardes, Santos-

Filho et al. 2008, Sartim, Costa et al. 2016), serine proteases (de Oliveira, de Sousa et al. 2016), L-amino acid oxidases (LAAOs) (Franca, Kashima et al. 2007), acidic PLA2s (Silveira, Marchi-Salvador et al. 2013) and Lys49 myotoxins (Soares, Andriao-Escarso et al. 2000), all of which likely contribute to the envenomation symptoms. Here we show that a specific venom component, a Lys49 myotoxin, can directly elicit pain and inflammation, as well as mechanical and heat hypersensitivity. As BomoTx action appears to be neural-specific and does not directly promote nerve damage, we hypothesize that these physiologic and behavioral effects of BomoTx are initiated by ATP release from BomoTx-sensitive primary afferent nerve terminals. The ATP released can activate $P2X_2$-and/or $P2X_3$-expressing nociceptors, as well as P2Y-expressing non-neural cell types, as observed in our culture system, where ATP released from neurons activates nearby fibroblasts. Subsequent release of inflammatory effectors (including purines) (Idzko, Ferrari et al. 2014), can then act back on nociceptors to generate inflammatory pain and hypersensitivity. For example, stimulation of TRPV1-positive fibers produces heat hypersensitivity, whereas activation of $P2X_2/P2X_3$-expressing fibers elicits mechanical hypersensitivity, consistent with roles for these nociceptor subtypes in thermal and mechanical pain, respectively (Tsuda, Koizumi et al. 2000, Honore, Kage et al. 2002).

Figure. 1 BomoTx activates two distinct subpopulations of sensory neurons

(A) Brazilian Lancehead, *Bothrops moojeni* (photo credit to Texas A&M University-Kingsville Office of Marketing and Communication). (B) Representative screen using ratiometric calcium imaging of cultured rat TG neurons. Crude snake venoms were analyzed before and after a filtration cleanup step to, in some cases, reveal specific responses by a subset of neurons (arrowheads). Subsequent response to high (150mM) extracellular K^+ reveals all neurons in the field. (C-D) BomoTx (1μM) elicited two types of responses characterized by large, sustained calcium responses in one group (C, pie chart blue slice, 3.26%) and small, transient calcium responses in another group (D, pie chart green slice, 6.98%). Representative images are shown above each trace, where arrowheads indicate BomoTx-sensitive neurons. (E) Non-neuronal cells (arrowheads) were activated in the vicinity of BomoTx-sensitive neurons showing sustained responses (arrow). They are characterized by transient calcium elevation with no response to high K^+. (F-G) Averaged calcium imaging traces of sustained (F, pie chart blue slice, 1.98%) and transient (G, pie chart green slice, 0.18%) BomoTx-sensitive neurons when apyrase (Apy, 20U) was co-applied with the toxin. The number in (F) is not significantly different from (C) while the number in (G) is significantly less than (D). **$P<0.01$, one-way ANOVA with post hoc Tukey's test. (H) Responses by non-neuronal cells (arrowheads) are seen only in the absence of apyrase and in close proximity to BomoTx-sensitive sustained neurons (arrow). (I-J) Quantification of toxin-responsive sustained (I) and transient (J) cells in P0 TG cultures showing the percentage of toxin-sensitive cells that also responded to other agonists (10nM capsaicin, 1μM AITC,

100µM menthol, 1µM Hm1a, 100µM ATP, 30µM α,β-MeATP) or bind the lectin IB4, and vice versa (n=3-10). (K) Size distribution of all P0 TG neurons (grey, 125 neurons counted) and BomoTx-sensitive sustained (blue, 37 neurons counted) or transient (green, 60 neurons counted) neurons. All data represent mean ± S.E.M.
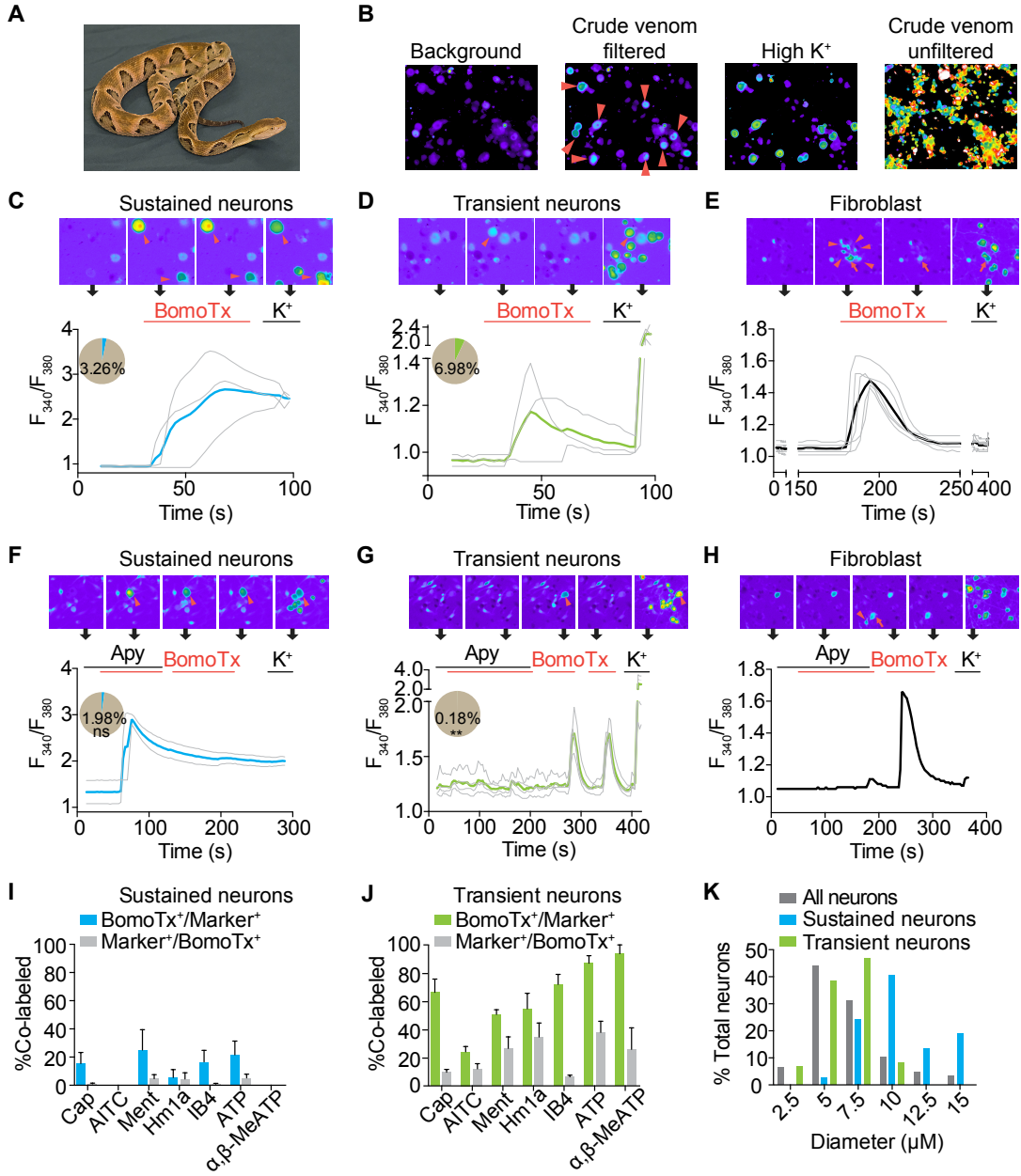
A

B

Background | Crude venom filtered | High K$^+$ | Crude venom unfiltered

C Sustained neurons

D Transient neurons

E Fibroblast

BomoTx   K$^+$

3.26%

BomoTx   K$^+$

6.98%

BomoTx   K$^+$

F Sustained neurons

G Transient neurons

H Fibroblast

Apy   BomoTx   K$^+$

1.98% ns

Apy   BomoTx   K$^+$

0.18% **

Apy   BomoTx   K$^+$

I Sustained neurons

- BomoTx$^+$/Marker$^+$
- Marker$^+$/BomoTx$^+$

Cap AITC Ment Hm1a IB4 ATP α,β-MeATP

J Transient neurons

- BomoTx$^+$/Marker$^+$
- Marker$^+$/BomoTx$^+$

Cap AITC Ment Hm1a IB4 ATP α,β-MeATP

K

- All neurons
- Sustained neurons
- Transient neurons

Diameter (μM)

47

Figure. 2 BomoTx-induced transient responses are mediated by ATP

(A) Representative current-voltage relationship of BomoTx (1µM)-evoked conductance from transiently activated TG neurons (whole cell configuration; baseline subtracted, each trace normalized to the current at -60mV) demonstrate inwardly rectified currents that reverse at 0mV (n=3). (B) Representative whole cell voltage clamp experiments on TG neurons showing that Ro51 (100nM) blocks BomoTx-evoked current. The same neurons also respond to ATP (100µM) and α,β-MeATP (30µM) (n=8). Vertical scale bars, 50pA; horizontal bars, 10s; V_{hold} = -60mV. (C) BomoTx does not directly activate HEK cells expressing rat $P2X_2$, $P2X_3$, or $P2X_{2/3}$ channels (n=7-11). Vertical scale bars, 0.5nA; horizontal bars, 10s. (D) Embryonic DRG culture transduced with lentivirus expressing rat $P2X_2$ (right trace) shows significantly increased percentage of BomoTx responsive cells (20.12%, n=30) compared to uninfected control culture (left trace) (2.98%, n=20). Responses to ATP (100µM) or α,β-MeATP (30µM) were also increased in $P2X_2$ transduced cultures (bottom). Each trace represents an individual neuron (n>300) with representative images shown above. Activities are quantified in the bottom. Apyrase (20U) significantly reduces BomoTx-induced calcium responses in $P2X_2$ transduced culture (1.71%, n=3). ***$P < 0.001$, ****$P < 0.0001$, one-way ANOVA with post hoc Tukey's test. Data are shown as mean ± S.E.M.
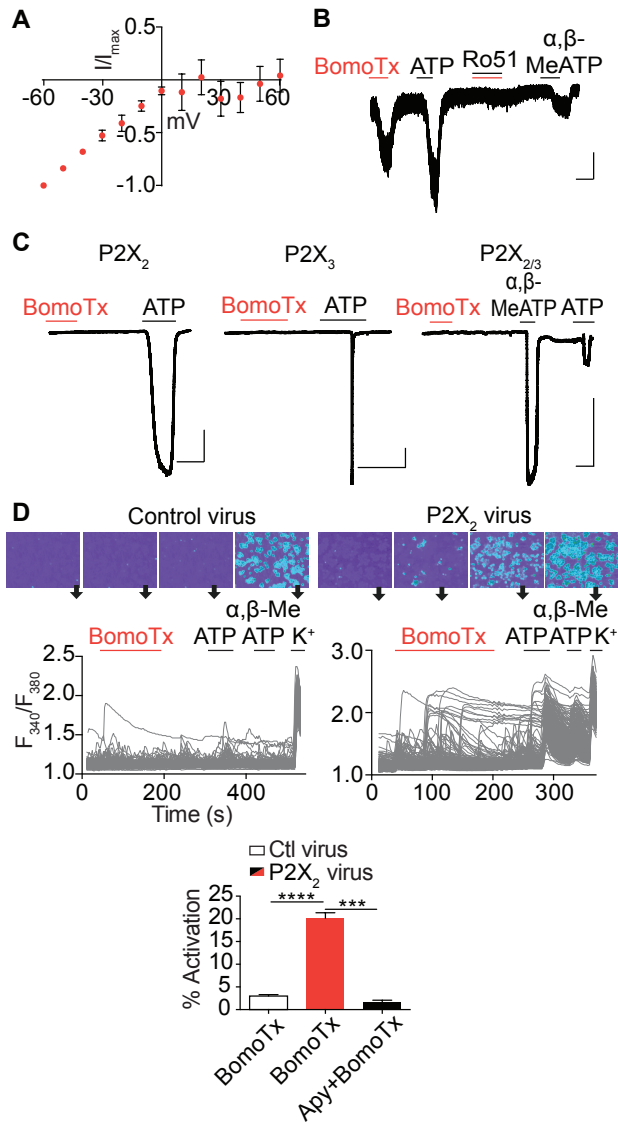
A

I/I_{max}

0.5

-60   -30   30   60

mV

-0.5

-1.0

B

BomoTx   ATP Ro51   α,β-
MeATP

C

P2X$_2$ P2X$_3$ P2X$_{2/3}$
α,β-
BomoTx   ATP   BomoTx   ATP   BomoTx MeATP ATP

D

Control virus   P2X$_2$ virus

α,β-Me   α,β-Me
BomoTx   ATP ATP K$^+$ BomoTx   ATP ATP K$^+$

2.5   3.0

F_{340}/F_{380}

2.0   2.0

1.5

1.0   1.0

0   200   400   0   100 200 300
          Time (s)

□ Ctl virus
■ P2X$_2$ virus

25
20   ****   ***
15
% Activation
10
5
0
   BomoTx   BomoTx   Apy+BomoTx

49

Figure. 3 BomoTx-induced ATP release requires hemichannels

(A) Calcium imaging traces showing example of BomoTx (1μM) application in P0 mouse TG culture (>70 neurons) with and without CBX (10μM). Blue traces and pie chart slice indicate sustained neurons (2.33% with CBX and 4.57% without CBX); green traces and pie chart slice indicate transient neurons (4.65% with CBX and 11.45% without CBX) (n=5). ****P<0.0001, one-way ANOVA with post hoc Tukey's test. (B) Representative images of neurons with sustained calcium responses (arrowheads) compared to those subsequently exhibiting YO-PRO-1 (0.1μM) uptake, showing complete (93.3 ± 16.3%) overlap (n=6). (C) (Left) Whole-cell patch recording from neurons showing sustained or transient calcium responses immediately after toxin application. 80% (4/5) of sustained neurons showed a CBX-sensitive current compared to none (0/5) of the transiently activated cells. Voltage steps are from -90 to 90mV with 20mV increment; holding potential is -70mV. Vertical scale bars, 1nA; horizontal bars, 100ms. (Right) Current-voltage relationship of CBX sensitive currents in BomoTx-evoked transient and sustained neurons. I_{CBX} is calculated by subtracting steady-state current at each voltage step from that in the presence of CBX. (D) Calcium imaging of BomoTx-evoked responses in the absence and presence of extracellular calcium. With EGTA and no extracellular calcium, a group of neurons (blue traces and arrowheads, thick trace is average of all blue traces) were activated; adding extracellular calcium subsequently activated another group of neurons (green traces and arrowheads). Note that addition of extracellular calcium also activates SOCE in the first group of neurons (n=20). (E) Co-application of apyrase (20U) and BomoTx did not affect toxin-evoked intracellular

calcium transients and SOCE (blue traces), but reduced the population of cells responding to subsequent extracellular calcium addition (grey traces) (n=32). (F) Pretreatment with tharpsigargin (Thg, 2µM, 5min) in the absence of extracellular calcium abolished all BomoTx responses. Subsequent addition of extracellular calcium activated SOCE in all cells (n=12). (G) Pretreatment with U73122 (U7, 10µM, 5min) in the absence of extracellular calcium abolished all BomoTx responses. (H) Quantification of the percentage of the calcium responses evoked by BomoTx under different calcium conditions. $*P < 0.05$; $**P < 0.01$, $****P < 0.0001$, one-way ANOVA with post hoc Tukey's test. (I) YO-PRO-1 staining immediately after BomoTx application in the absence and then presence of extracellular calcium. Calcium imaging example is from (D); blue and green arrowheads indicate cells with intracellular calcium release and extracellular calcium responses, respectively. Note that only cells with intracellular calcium release have YO-PRO-1 staining. Pie charts show percentage of YO-PRO-1 positive neurons (green) for those exhibiting BomoTx-evoked intracellular calcium release (left) versus extracellular calcium influx (right) (n=4). (J) Proposed mechanism of BomoTx action in neurons. BomoTx targets sensory neurons through an unknown receptor, which activates intracellular calcium release leading to subsequent pannexin hemichannel opening, YO-PRO-1 permeation and ATP release. The released ATP then activates sensory neurons that express ionotropic $P2X_2$ and $P2X_3$ receptors, as well as P2Y metabotropic receptors on fibroblasts.
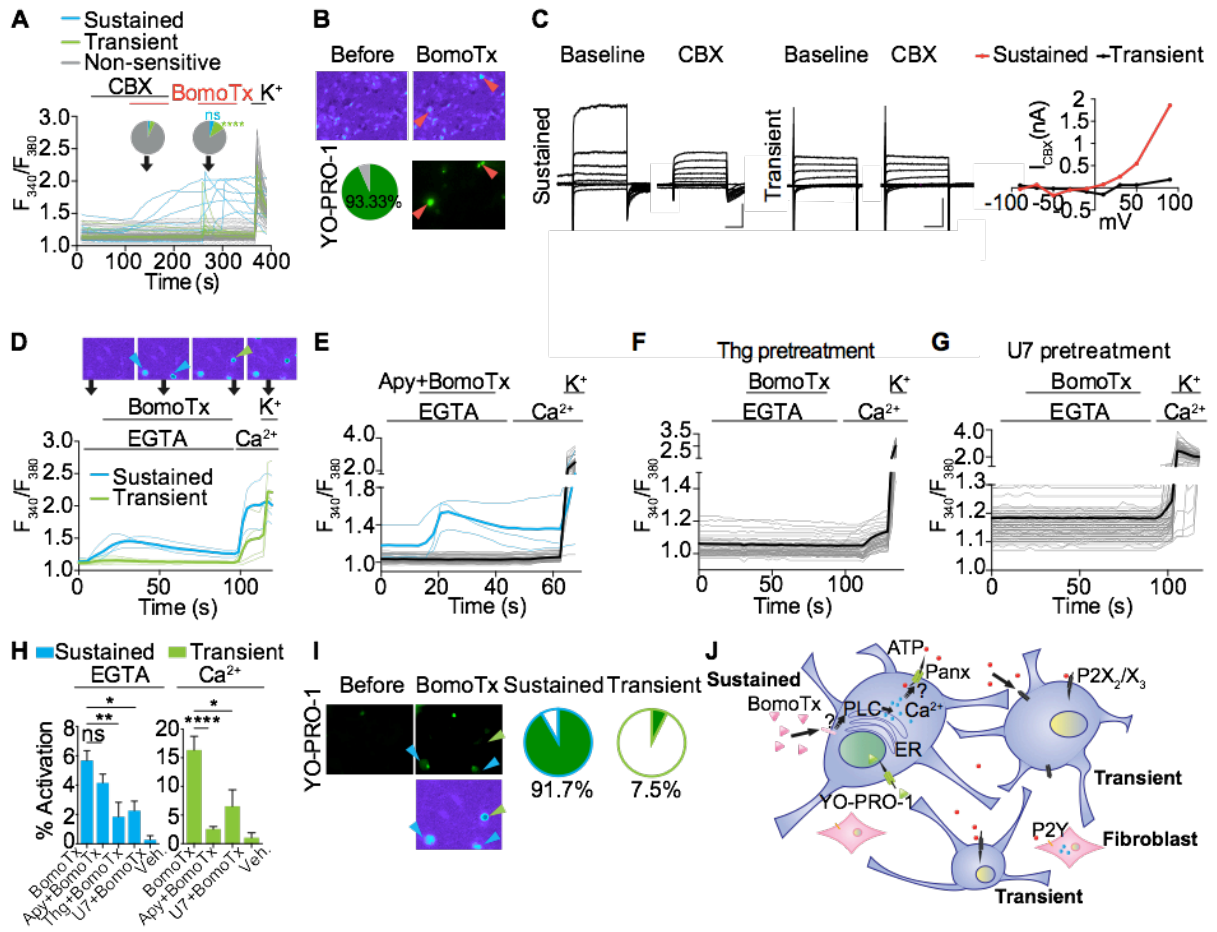
Figure. 4 BomoTx evokes pain and produces thermal and mechanical hypersensitivity

(A) Comparison of licking behavior following intraplantar injection of BomoTx (50µM in 20µl 0.1%BSA) (n=7) versus vehicle (n=4). Nocifensive behavior was not significantly reduced in $P2X_2/P2X_3^{dbl-/-}$ (DKO) mice (n=6) but was significantly decreased after ablation of TRPV1-expressing terminals in the spinal cord by intrathecal capsaicin (I.T. cap) injection in WT(n=10) and DKO mice (n=3). (B-C) Quantification and representative images of Fos protein immunostaining in superficial laminae of spinal cord sections from toxin-injected mice ipsilateral (Ipsi.) or contralateral (Contr.) to the injected hindpaw (sections n=80 for WT and DKO, 30 for I.T. cap, 20 for I.T. cap DKO and control). Scale bar, 100µm. (D) Latency of paw withdraw from noxious heat stimulus measured in WT (n=6), DKO (n=6) and I.T. cap (n=7) mice 15min after BomoTx (5µM) or vehicle (n=3) injection. (E) Mechanical threshold for WT or DKO mice (n=8 each) 15min after vehicle or BomoTx intraplantar injection. (F) Evans blue dye (EBD) extravasation measured in BomoTx- or capsaicin (5µM)-injected paw compared to contralateral controls in WT and $PPTA^{-/-}$ mice (n=3 for all BomoTx injections, n=7 for WT cap injection). (G) Proposed mechanism of BomoTx-evoked pain. BomoTx releases ATP from nerve endings through hemichannels, directly activating P2X and/or P2Y-expressing sensory neurons, as well as non-neural cells (e.g. keratinocytes, mast cells, local immune cells) that release inflammatory mediators (such as bradykinin, H^+ and more ATP), in turn activating sensory nerve fibers. Activation and sensitization of TRPV1-positive fibers produces acute inflammatory pain and thermal hypersensitivity, whereas activation of $P2X_2$ and $P2X_3$ fibers elicits acute pain and mechanical hypersensitivity. For all, *P<0.05;

**P<0.01, ***P<0.001, ****P<0.0001, one-way ANOVA with post hoc Tukey's test. Data are shown as mean ±S.E.M.
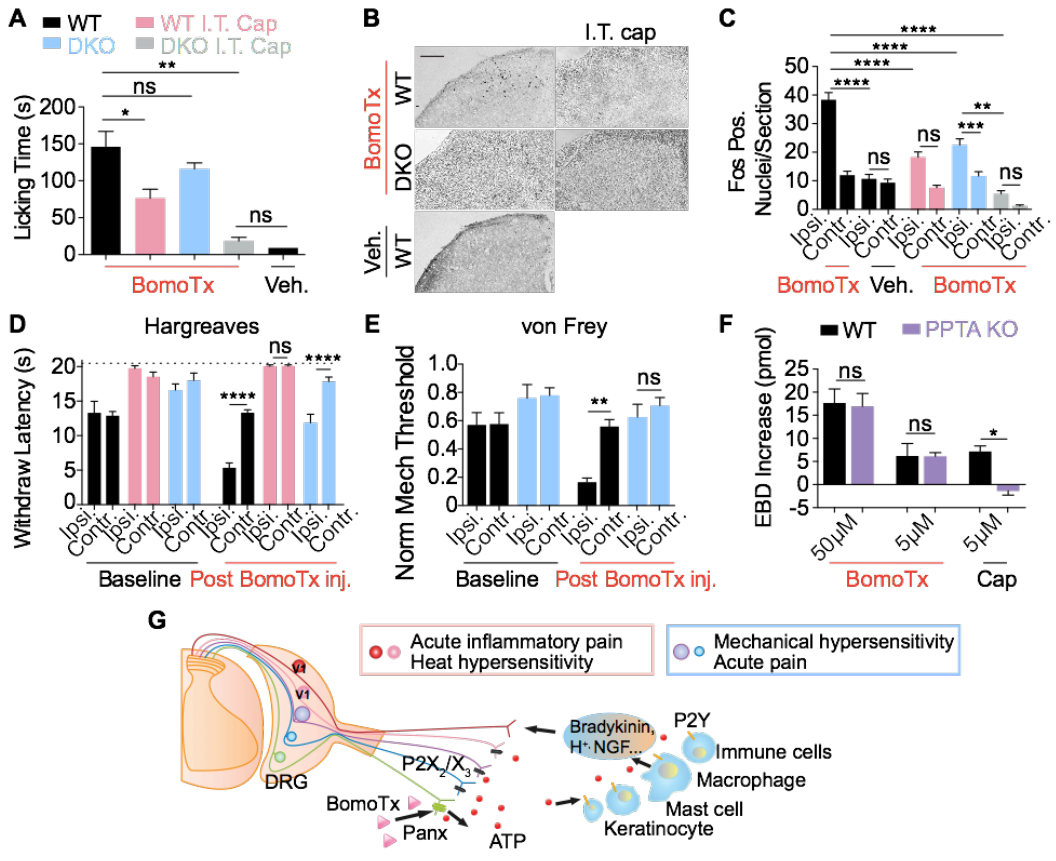
A

WT ■   WT I.T. Cap ■
DKO ■   DKO I.T. Cap ■

Licking Time (s)

BomoTx   Veh.

B

I.T. cap

BomoTx: WT, DKO

Veh.: WT

C

Fos Pos. Nuclei/Section

Ipsi. Contr. Ipsi. Contr. Ipsi. Contr. Ipsi. Contr. Ipsi. Contr.
BomoTx   Veh.   BomoTx

D

Hargreaves

Withdraw Latency (s)

Ipsi. Contr. Ipsi. Contr. Ipsi. Contr. Ipsi. Contr. Ipsi. Contr. Ipsi. Contr.
Baseline   Post BomoTx inj.

E

von Frey

Norm Mech Threshold

Ipsi. Contr. Ipsi. Contr. Ipsi. Contr. Ipsi. Contr.
Baseline   Post BomoTx inj.

F

WT ■   PPTA KO ■

EBD Increase (pmol)

50 μM   5 μM   5 μM
BomoTx   Cap

G

Acute inflammatory pain
Heat hypersensitivity

Mechanical hypersensitivity
Acute pain

V1

DRG

P2X$_2$/X$_3$

BomoTx

Panx

ATP

Bradykinin, H$^+$, NGF...

P2Y

Immune cells

Macrophage

Mast cell

Keratinocyte

55

Figure. 5 Identification of BomoTx

(A) Venom fractionation by semi-prep reversed-phase HPLC revealed one peak (red asterisks) exhibiting excitatory activity. The active peak was collected and purified by analytical HPLC to give a pure single active fraction. (B) BomoTx lacks sPLA2 enzyme activity compared with active bee sPLA2. Sequences above show comparison of BomoTx and bee sPLA2, with active site resides highlighted in blue. Note the lack of key aspartate residue (red) in BomoTx. (C) MALDI-TOF mass spectrometry profile of purified BomoTx. Only ions corresponding to BomoTx were observed. While the major peak represents the MH^+ ion cluster, the polypeptide was also detected doubly charged, and the determined molecular mass was ~13,835 Da. (D) MALDI-TOF mass spectrometry profiles of input BomoTx, BomoTx after 24hr protease digestion and BomoTx 24hr control. Peaks representing BomoTx are highlighted in red; other peaks represent standards. (E) Coomassie blue staining of protein gel that contains input BomoTx, BomoTx after different hours of protease digestion and BomoTx with no protease control. The dotted band indicates the size corresponding to BomoTx. (F-G) 24hr digested BomoTx (1µM) elicited no responses in cultured TG neurons (pie chart black slices). Non-digested BomoTx could still evoke two types of responses: sustained calcium responses (F, pie chart blue slice, 3.77%) and transient calcium responses in another group (G, pie chart green slice, 5.06%). Representative images are shown above each trace, where arrowheads indicate BomoTx-sensitive neurons. (H) Sequence alignment of identified BomoTx from *Bothrops moojeni*, with highly similar myotoxins M1-3-3 from *Bothrops asper*, MjTx-II and MjTx-I from *Bothrops moojeni*.
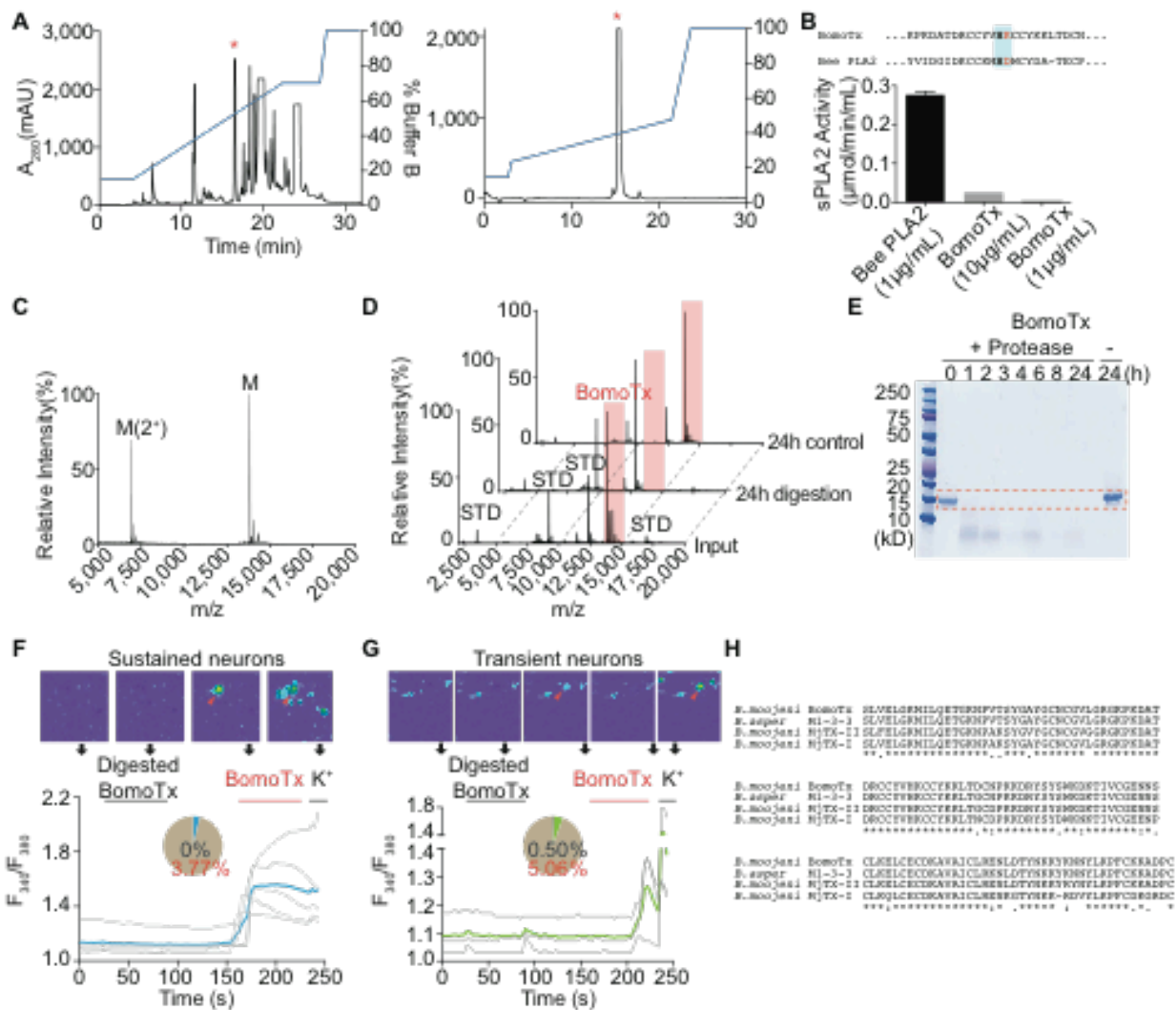
Figure. 6 Functional overlap with other somatosensory markers

(A) Representative calcium imaging traces showing individual P0 mouse TG neurons responding to BomoTx (1μM) in a sustained or transient manner, and either responded or did not respond to agonists (10nM capsaicin, 1μM AITC, 100μM menthol, 1μM Hm1a, 30μM α,β-MeATP and 100μM ATP). n=3-9. (B) Calcium imaging examples showing locations of transiently activated fibroblasts. Note that only those in close proximity to the sustained BomoTx-responding neuron (arrow) were activated. The high K^+ response of these cells is shown in Figure. 1E.

A

— BomoTx sustained only   — BomoTx sustained & marker
— BomoTx transient only   — BomoTx transient & marker

B

Background   BomoTx
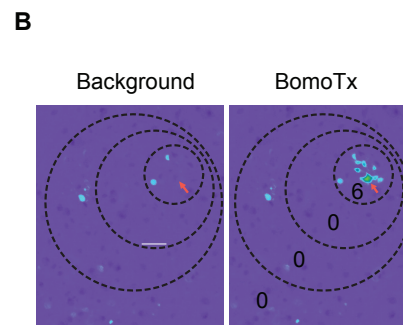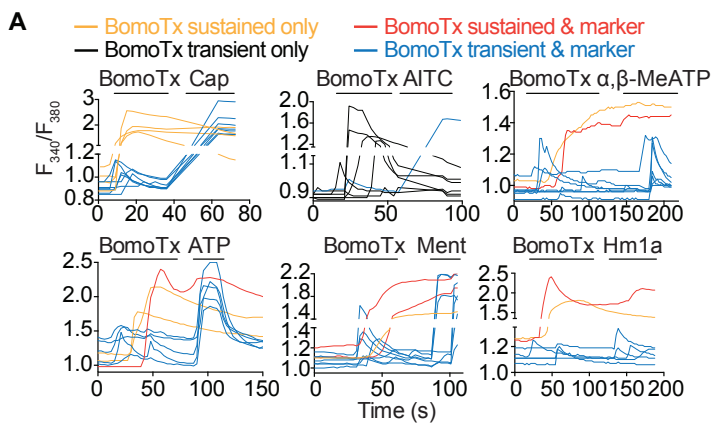
Figure. 7 BomoTx cytotoxicity and specificity in sensory neurons

(A) In HEK cell expressing $P2X_2$ or $P2X_{2/3}$, dose–responses of ATP-evoked currents are comparable to those evoked by co-applications of ATP and BomoTx (1µM). Currents are normalized to the maximal current in response to combined ATP and BomoTx. Data were fitted to the Hill equation (n=9). (B) Representative calcium imaging traces showing responses to BomoTx in $P2X_2$-transduced embryonic DRG neuronal culture with and without apyrase (20U). (C) Embryonic DRG responses to BomoTx after 4 days of culture. Typical BomoTx-induced responses are observed as seen in P0 culture. However, reduced BomoTx responses are seen after 10 days of culture (Fig. 2D). This is caused by reduced expression of $P2X_2$ (data not shown) and hence ATP responses caused by BomoTx. (D) BomoTx LD_{50} in sensory neurons (TG or DRG) and HEK cells measured to be 10µM and 50µM, as determined by CytoTox-Glo^{TM} luminescence assay (n=5). (E) Quantification of BomoTx-induced calcium responses in various cell lines or primary cell cultures (n=3-4). HPC, hippocampal culture. HPC and TG responses are normalized to total high K^+ responses; all others are normalized to total ATP responses. Notice that only hippocampal culture, sensory neuron culture and C2C12 myotubes responded robustly to BomoTx at either 1µM or 10µM concentrations.

A

P2X$_2$

P2X$_{2/3}$

B P2X$_2$ virus

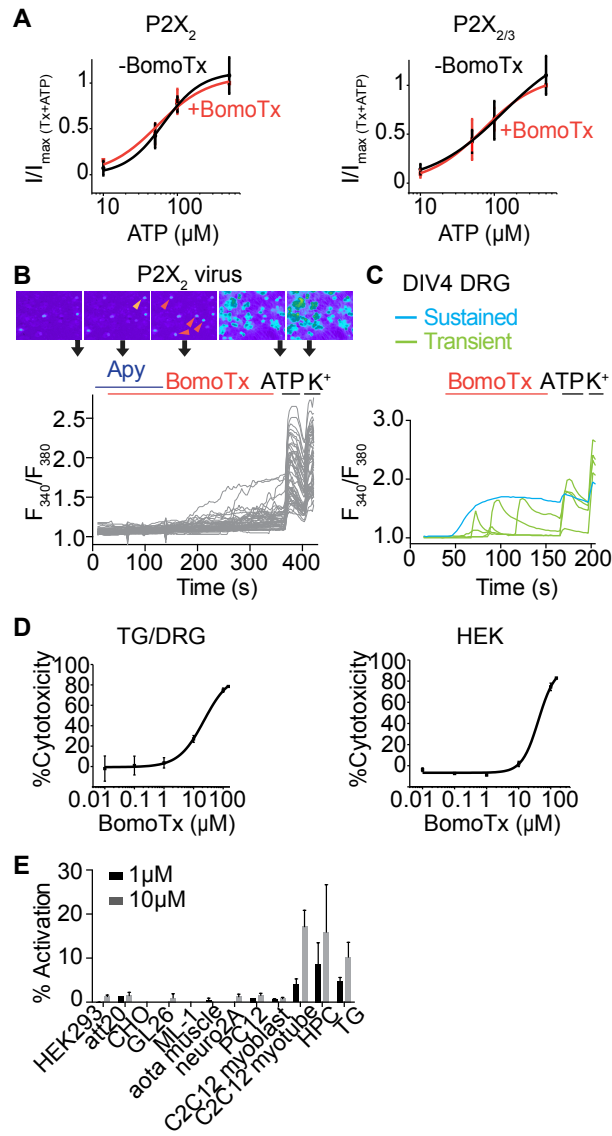**C** DIV4 DRG

D TG/DRG

HEK

E

61

Figure. 8 BomoTx-induced ATP release through hemichannels in neurons

(A) Quantification of the percentage of NeuN and DAPI positive cells compared with NeuN negative, DAPI positive (white arrowhead) and α-GFAP and DAPI positive (yellow arrowhead) cells (n=8). More than 200 cells per experiment were counted. Red, NeuN; green, α-GFAP; blue, DAPI. (B) N-ethylmaleimide (NEM), monensin (Mon) and tetanus toxin long chain lentiviral transduction (TeTx) do not reduce BomoTx-responding neurons in calcium imaging (n=3-15). (C) Carbenoxolone (CBX), niflumic acid (NFA) and flufenamic acid (FFA) can significantly reduce BomoTx-induced calcium responses in a dose-depended manner (n=3-9). (D) Calcium imaging traces of BomoTx responses in $P2X_2$ transduced embryonic DRG culture with and without CBX (10µM) (n=3). (E-F) HEK cells expressing pannexin1 (E, n=3) or pannexin1/2 (F, n=3) show no responses to BomoTx at 1µM. Vertical scale bars, 0.1nA; horizontal bars, 100ms. (G) In embryonic DRG culture transduced with lentiviral $P2X_2$, BomoTx-induced neuronal activation in the presence and absence of pan-caspase inhibitor Z-VAD-FMK (100µM) (n=12).
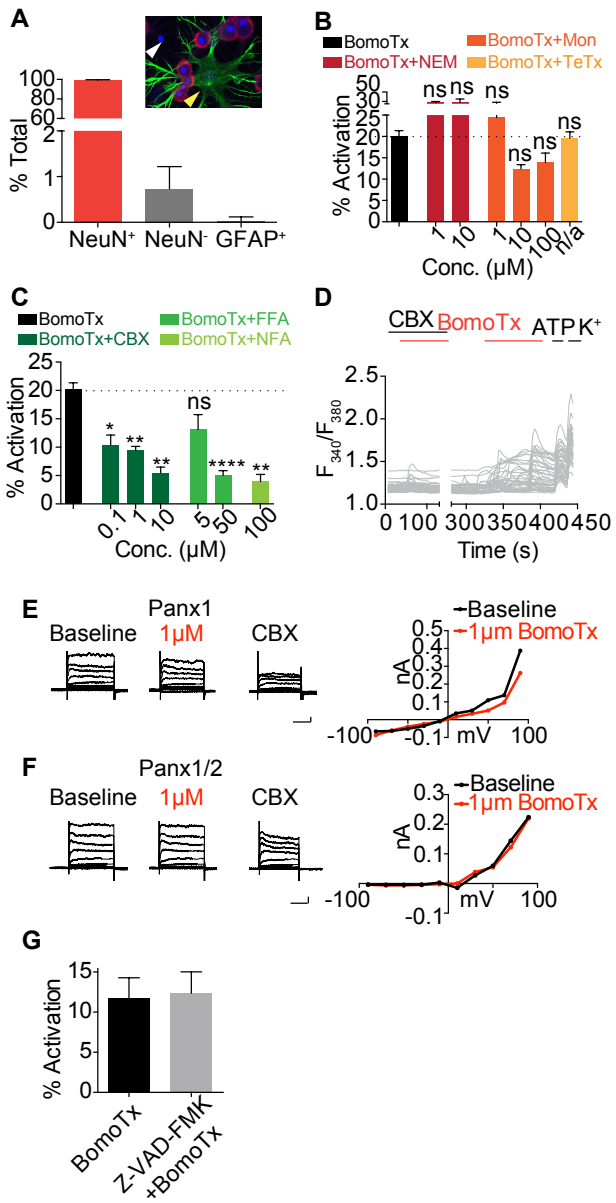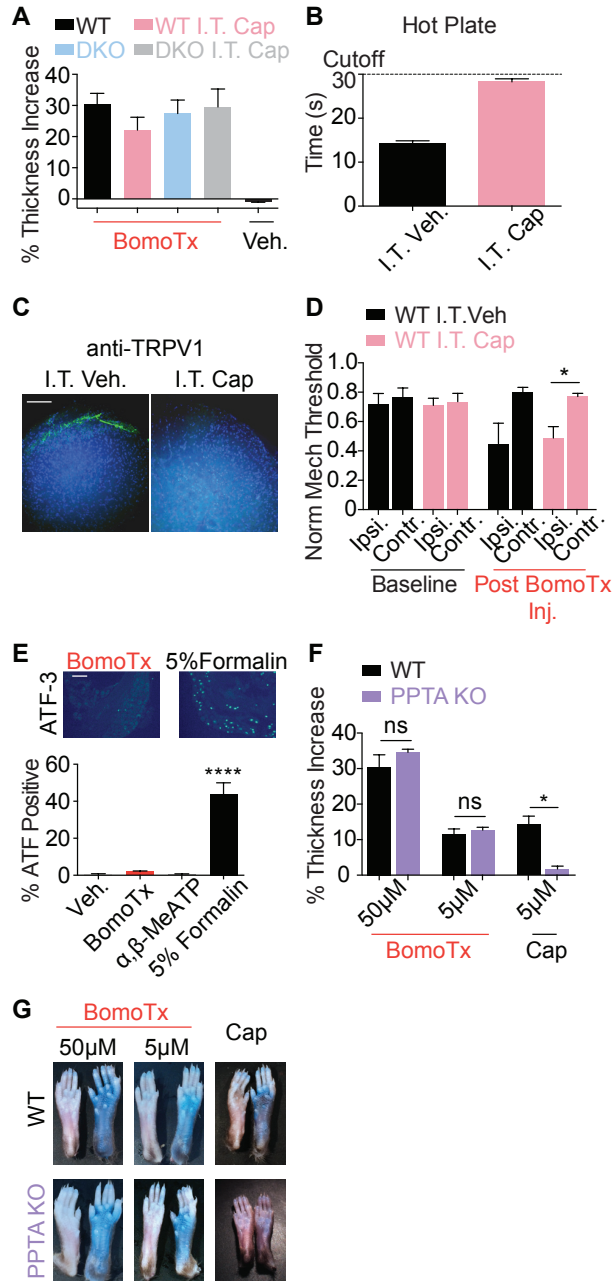
Figure. 9 Behavioral effects after BomoTx injection

(A) Paw thickness increases following intraplantar injection of BomoTx in WT, DKO, WT I.T. Cap and DKO I.T. Cap mice (n=3 each). Paw thick was quantified by the injection-induced increase in the ipsilateral versus contralateral hindpaws. (B) Latency of nocifensive behaviors in mice after I.T. vehicle (n=4) or I.T. cap (n=8) in hot plate test (plate set at 55°C). (C) Immunostaining of TRPV1 in the superficial laminae dorsal horn in lumbar spinal segment from I.T. cap or I.T. vehicle mice. (D) Mechanical threshold of mice after I.T. cap (n=8) or I.T. vehicle (n=4) measured before and after intraplantar BomoTx (5µM). (E) ATF3 induction in DRG following intraplantar 5% formalin, BomoTx (50µM), α,β-MeATP (100µM) or vehicle injection (measured 3 days post-injection, n=3 each). (F) Paw thickness increases after BomoTx or capsaicin injection (n=3 for all BomoTx injections, n=7 for WT cap injection) in WT and PPTA$^{-/-}$ mice. (G) Representative images comparing EBD extravasation in BomoTx- or cap-injected and in contralateral (uninjected, control) paws in WT and PPTA$^{-/-}$ mice.

A

WT ■ WT I.T. Cap ■
DKO ■ DKO I.T. Cap ■

% Thickness Increase

BomoTx   Veh.

B

Hot Plate

Cutoff

Time (s)

I.T. Veh.   I.T. Cap

C

anti-TRPV1

I.T. Veh.   I.T. Cap

D

WT I.T.Veh ■
WT I.T. Cap ■

Norm Mech Threshold

*

Ipsi. Contr. Ipsi. Contr.   Ipsi. Contr.

Baseline   Post BomoTx
Inj.

E

ATF-3   BomoTx   5%Formalin

% ATF Positive

****

Veh.   BomoTx   α,β-MeATP   5% Formalin

F

WT ■
PPTA KO ■

% Thickness Increase

ns   ns   *

50μM   5μM   5μM

BomoTx   Cap

G

BomoTx

50μM   5μM   Cap

WT

PPTA KO

65

Acknowledgement

CHAPTER 4

Tanzanian Blue Ringleg Centipede Toxins Reveal Evolutionary Connection With Potassium Channel Blocker A-Scorpion Toxins

Introduction

Despite the incredible diversity of venomous animals, most toxins characterized to date derive from a relatively small group of species. An under-studied group is represented by centipedes, which belong to the oldest terrestrial venomous lineage after scorpions (Undheim, Jones et al. 2014). Centipedes are, indeed, highly venomous and their bites are known to produce pain and are even capable of killing small animals (Balit, Harvey et al. 2004). Hence, studying their venom could potentially help to reveal new pain mechanisms.

Recent studies show that centipede venoms are unlike those from other arthropods such as spiders and scorpions (Undheim, Sunagar et al. 2014, Undheim, Jenner et al. 2016). Centipedes contain many novel toxin families that are of unknown structure and function (Liu, Zhang et al. 2012, Yang, Liu et al. 2012). Discovering and characterizing these novel toxins could provide a better understanding of protein neofunctionalization and evolutionary relationships among different animal groups (Undheim, Jones et al. 2014).

Here, I will describe the discovery of centipede toxins μ-SLPTX$_{15}$-Sm1a/b (henceforth Sm1a/b). They were initially discovered based on their ability to activate subpopulations of sensory neurons. Sequence analysis and NMR structural studies have revealed that Sm1a/b form a novel CS$\alpha\beta$ fold, much resembling the scorpion defensin and K$^+$ channel

blocking toxins, α-KTxs (Miller 1995, Rodriguez de la Vega and Possani 2004, Luna-Ramirez, Bartok et al. 2014, Meng, Xie et al. 2016).

Results

A novel toxin that targets somatosensory neurons

We used live-cell calcium imaging to screen a library of 100 arthropods venoms including centipedes, scorpions and spiders for their ability to activate primary sensory neurons cultured from rat trigeminal ganglia (TG), as previously described in Chapter 3. After processing raw venoms with a molecular weight cutoff filter, we identified *Scolopendra morsitan* (Figure. 10A) venom as an interesting candidate that robustly activated a subpopulation of TG neurons. Fractionation of this crude venom by reversed phase (C_{18}) chromatography yielded two neighboring active peaks (Figure. 10B, C), each of which could recapitulate the activity observed with the crude filtered venom.

To reveal the toxins' identities, active fractions from these adjacent peaks were proteolytically digested and analyzed with MALDI-TOF mass spectrometry. Results were searched against *Scolopendra morsitan* venom gland transcriptome (Undheim, Sunagar et al. 2014), identifying μ-SLPTX$_{15}$-Sm1a/b (Sm1a/b) as the active components (Figure. 10D). Sm1a and b sequences closely resemble one another, differing by only one amino acid. An inactive HPLC fraction preceding Sm1a/b contains another toxin, named Sm2, which also belongs to the Sm1a/b family and shares the same disulfide

pattern (Figure. 10D). This disulfide pattern (CXXXC…CXC) is distinct from any known toxin protein families, thus representing a novel toxin family from this centipede.

Sm1a/b elicits robust calcium responses in a subpopulation of cultured TG neurons (about 12%) (Figure 11A). These calcium responses show a "twinkling" pattern characterized by rounds of rapid free-calcium fluctuation during toxin application. This twinkling pattern might indicate possible involvement of voltage-gated ion channels, such as that observed with the Hm1a toxin, which targets Nav1.1 (Osteen, Herzig et al. 2016). To test whether sodium channels might also be involved in Sm1a/b-evoked neuronal activation, I applied these toxins to TG neurons in the presence of lidocaine and TTX. These sodium channel antagonists did not block Sm1a/b-evoked calcium responses, indicating that sodium channels are not directly involved (Figure. 11B, C). In addition, ruthenium red, which blocks many TRP channels and some calcium channels, was also ineffective at blocking toxin-evoked neuronal activation (Figure. 11D). Hence, Sm1a/b induced calcium transients in sensory neurons through a mechanism that might involve voltage-gated channels but not sodium channels or several TRP channel and calcium channel subtypes that are ruthenium red-sensitive.

Sm1a structure reveals potential Kv channel toxins

As centipedes produce only a small amount of venom, synthetic peptides corresponding to the native toxin must be made to fully characterize toxin properties. Sm1a was then synthesized using Fmoc chemistry, and disulfide bond formation was initially achieved

with random oxidation using NH_4HCO_3. The three resulting disulfide isomers of Sm1a were purified using RP-HPLC, and only one specific isomer co-eluted with native Sm1a and adopted a well-defined tertiary structure. We thus conclude that this 1-3, 2-4 disulfide isomer likely corresponds to native Sm1a. Further tryptic digestion experiments have shown that both synthetic and native Sm1a have identical digestion patterns that co-elude in RP-HPLC, hence revealing that no L- to D-amino acid conversion exists in the native Sm1a. Hence, this peptide should structurally recapitulate native Sm1a.

As the Sm1a sequence predicts a novel disulfide fold, we then used NMR to resolve the synthetic Sm1a solution structure. Interestingly, Sm1a shows a nearly identical polypeptide backbone with a group of scorpion α-KTxs, both of which form a typical CSαβ fold with a two- or three-turn α-helix affixed to a three-stranded β sheet via a disulfide bond (Figure 12B). However, unlike these scorpion α-KTxs (for example, Charybdotoxin) that require three disulfide bonds to maintain the structural rigidity, Sm1a only uses two disulfide bonds. The first pair of disulfide bond in Charybdotoxin is potentially replaced with electrostatic interactions of Lys12 and His43 in Sm1a (Figure. 12B), thus stabilizing the N-terminus of the α-helix. Thus, Sm1a utilized a new strategy to generate a conserved CSαβ toxin fold.

In light of the structural similarities between scorpion α-KTxs and Sm1a, we asked whether there is functional relevance between these two toxins. Charybdotoxin has been shown to block $Kv_{1.1}$ via the highly conserved Lys27 to occlude the outer entryway

to the K^+ conductance pore. Additional residues (for example, Tyr36) determine the affinity of the toxin for $Kv_{1.1}$ (Miller 1995, Rodriguez de la Vega and Possani 2004). These residues could also be found in cognate locations in Sm1a, namely Lys37 and His49, as seen in structure overlays with Charybdotoxin (Figure. 12C). This indicates potential functional roles of Sm1a in blocking potassium channels. However, when Sm1a was applied to cells expressing various Kv channel subtypes, no effects were observed (Figure. 13). This is not a complete screen of all reported α-KTx targets, and hence further experiments with a larger representation of Kv channels should be performed (see discussion below).

Discussion

We have discovered a novel centipede toxin that activates somatosensory neurons. This toxin, Sm1a, resembles scorpion α-KTxs in having a conserved CSαβ fold. However, the different disulfide bond patterns in Sm1a represent a new form of CSαβ fold unique to centipedes. The structural similarities suggest potential Sm1a function as a Kv channel blocker, although this has not been substantiated by functional analysis. So far, this study has revealed an evolutionary connection of a new family of centipede toxins to scorpion toxins, shedding light on the origins and diversities of the CSαβ fold.

Origins of CSαβ fold

The CSαβ fold, which has a conserved core cysteine framework of C[1]…C[2]XXXC[3]…C[4]…C[5]XC[6], is one of the most prevalent peptide folds,

accounting for 19% of all known peptide structures (Undheim, Mobli et al. 2016). In addition, the CSαβ fold has extremely widespread taxonomic distribution ranging from fungi (Wu, Gao et al. 2017) to plants (Vriens, Cools et al. 2016) and animals (Landon, Sodano et al. 1997, Rodriguez de la Vega and Possani 2004, Sugiarto and Yu 2004, Luna-Ramirez, Bartok et al. 2014). This raises the question of whether the CSαβ fold originates from a single origin, or has been independently recruited multiple times. To answer this question, it is important to survey multiple peptide structures with a CSαβ fold from different taxonomies. However, many studies only use peptide cysteine sequences as an alternative for CSαβ structure. Without structure analysis, alterations in the cysteine framework that do not change the overall fold could have led to misalignment of cysteines and obscured evolutionary links. Indeed, Sm1a lacks the first and fourth cysteines, but nonetheless forms a CSαβ fold, attesting to the importance of not relying solely on sequence data to study evolutionary relationships among peptide toxins. Furthermore, our findings suggest that separate evolutionary events have led to the formation of centipede CSαβ folds in arthropods. Further analysis of gene structures could help to investigate similarities and differences among these peptides and clarify such questions.

Unique properties stabilizing centipede CSαβ fold

The formation of CSαβ fold depends on the core motifs (CXXXC…CXC) to provide precise disulfide bridge locations for stabilizing the structure (Wu, Gao et al. 2017). The additional disulfide bridge, usually between the first and fourth cysteine linking the N-

terminus to the first β-strand, is also important for the maintaining the structure. Variations of the CSαβ fold often include additional disulfide bridge pairs (Rodriguez de la Vega and Possani 2004, Wu, Gao et al. 2017), but decreasing the number of disulfide bridges is rare (Song, Gilquin et al. 1997), possibly due to the lack of structural stability. In the case of Sm1a, a new structural strategy has to evolve in order to replace the lack of one disulfide bridge: the possible electrostatic interactions between of Lys12 and His43 may serve as a surrogate for the third pair of disulfide bridge normally seen in CSαβ fold. Hence, this toxin provides insight into a new form of CSαβ fold that likely employs only two disulfide bonds with electrostatic interactions.

Caveats with synthetic and native Sm1a toxins

In this study, we have made synthetic Sm1a that show many identical properties to the native Sm1a toxins, including 1) sequence, molecular weight, disulfide bridges and HPLC elution profiles, 2) lack of L- to D- modification (Buczek, Yoshikami et al. 2005) and other obvious post-translational modifications frequently seen in toxins (such as C-amidation). Hence, we have confidence that our studies reflect the true native Sm1a overall structure. However, this synthetic Sm1a does not recapitulate the neuronal excitation observed in native Sm1a fractions. It could be due to two reasons: 1) The native Sm1a fraction contains a small molecule or peptide that are responsible for the neuronal activation but not Sm1a *per se*; 2) The native Sm1a has some obscure post-translational modifications or co-factors that are hard to be detected in our methods. To address the first possibility, it is important to analyze the Sm1a venom fraction in the

small molecule or peptide range in the MALDI-TOF experiment, as our current experiment could only detect molecules larger than 1kD.

Figure. 10 Identification of Sm1a/b

(A) Centipede *Scolopentra morsitan*. (B) Venom fractionation by semi-prep reversed-phase HPLC revealed two peaks (red asterisks) exhibiting excitatory activity. (C) The active peaks were pooled and purified again by analytical HPLC, resulting in two relatively pure active factions (red asterisks). (D) Mature protein sequence alignment of Sm1a, Sm1b and Sm2. Cys residues are highlighted in blue and conserved sequences are in red.

A

B

C

D
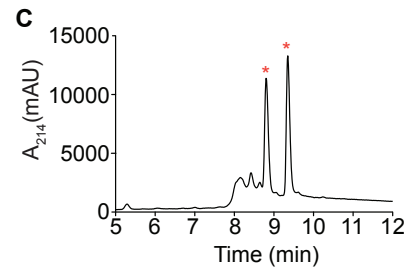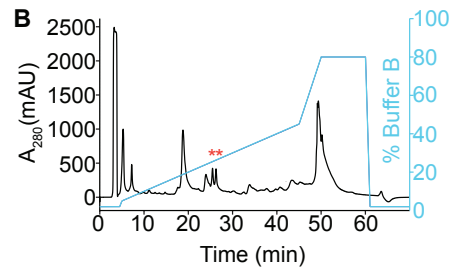
```
5996 Sm1a   --EETEEPIRHAKKNPSEGECKKACADAFANGDQSKIAKAENFKDYYCNCHIIIH 53
5980 Sm1b   --EETEEPIRHAKKNPSEGECKKACADAFANGDQSKIAKAENFKDFYCNCHIIIH 53

6009 Sm2    GKPEKEVNFPAPGKKPTREDCKKACANKYTNGVMSKVIVAK-LTGKNCYCKYQEN 54
```

Figure. 11 Native Sm1a/b-containing fraction excites a subpopulation of somatosensory neurons

(A) Calcium imaging traces and representative images of Sm1a fraction on cultured mouse TG neurons. Subsequent response to high (150mM) extracellular K^+ reveals all neurons in the field. Each trace represents a responding individual neuron and the thick black trace is average of all individual traces. Arrowheads indicate specific responses by a subset of neurons. (B-D) Calcium imaging traces of cultured TG neurons in response to Sm1a fractions in the presence of Lidocaine (1mM, B), TTX (500nM, C) or Ruthenium Red (10μM, D). (E) Quantification of the percentage of activated neurons in the presence and absence of blockers. None of the blockers could significantly block the toxin responses.
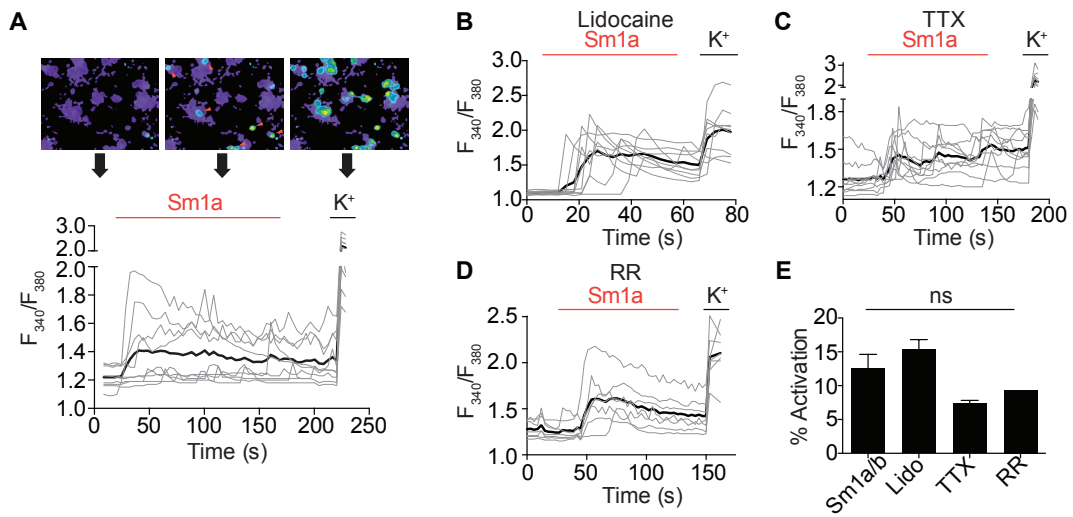
A

B Lidocaine
Sm1a K$^+$

C TTX
Sm1a K$^+$

D RR
Sm1a K$^+$

E ns

Figure. 12 Synthetic Sm1a structure

(A) Mature protein sequence alignment of Sm1a to scorpion α-KTxs. Cys residues are highlight in red. The key Lys residues for many of these α-KTxs to block potassium channels are in the blue rectangle. (B) NMR structural comparisons of Charybdotoxin (PDB: 2CRD) and synthetic Sm1a. Disulfide bonds are highlighted in yellow. Note the similarities of structure compositions and disulfide bond locations between the two toxins. The residues Lys12 and His43 for disulfide surrogate in Sm1a are highlight in deep blue and red, respectively. (C) Structure overlay of Charybdotoxin (silver) and Sm1a (green). Key residues in Charybdotoxin for blocking potassium channels (Lys27 and Tyr36) are highlighted. In Sm1a, Lys37 and His49 can be found in similar space of Charybdotoxin, which may indicate potential potassium blocking functions.

A

| | 10 | 20 | 30 | 40 | 50 |

Sm1a/1-53   EETEEPIRHAKKNPSEGECKKACADAFANGDQSKIAKAENFKDYYCNCHILIH
Charybdotoxin/1-37   -----QFTNVSC-TTSKECWSVCQRL---HNTSRG-KCMN-KK--CRCYS---
Noxiustoxin/1-39   -----TIINVKC-TSPKQCSKPCKELT--GSSA-GAKCMN-GK---CKCYNN--
Agitoxin1/1-38   ----GVPINVKC-TGSPQCLKPCKD---AGMRF-G-KCIN-GK--CHCTPK--
BmKDfsin4/1-37   ---------GFGCPFNQGQCHKHCGSIRRRG----G-YCDGFLKTRCVCYR--
TsTXKa/1-37   -----VFINAKC-RGSPECLPKCKEAI--GKAA-G-KCMN-GK---CKCYP--
BmPO5/1-31   ---------AVC--NLKRCQLSCRSL---GLL--G-KCIGD-K--CECVKH--
Maurotoxin/1-34   --------VSC-TGSKDCYAPCRKQT--GCP--NAKCIN--KS-CKCYGC--
PiTx-Ka/1-35   --------TISC-TNPKQCYPHCKKET--GYP--NAKCMNR-K--CKCFGR--
Cobatoxin1/1-32   --------AVC--VYRTCDKDCKRR---GYRS-G-KCINNA---CKCYPY--
Psp/1-37   ----DEEPKESC--SDEMCVIYCKGEE--YST-GV-CDGPQK--CKCSD---
Butantoxin/1-40   --WCSTCLDLAC-GASRECYDPCFKAF--GRAH-G-KCMNN-K--CRCYT--
Tc1/1-23   ----------AC----GSCRKKCK------GS---G-KCINGR---CKCY---
Bmkk1/1-31   ----TPFAIKC-ATDADCSRKCP-----GNPS---CRNGF---CACT----
AaTx1/1-37   ----QIETNKKC--QGGSCASVCRRVI--GVAA-G-KCINGR---CVCYP--
Martentoxin/1-37   ----FGLIDVKC-FASSECWTACKKVT--GSGQ-G--KCQNNQ---CRCY----

B
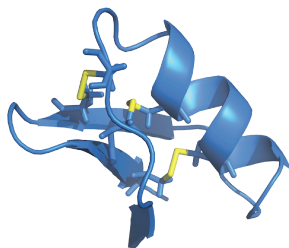
Charybdotoxin   Sm1a
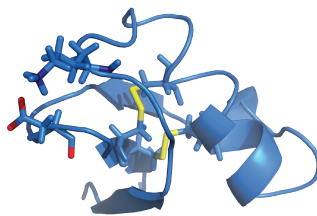
C

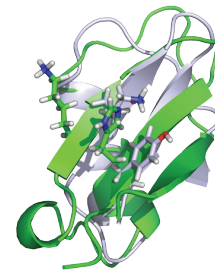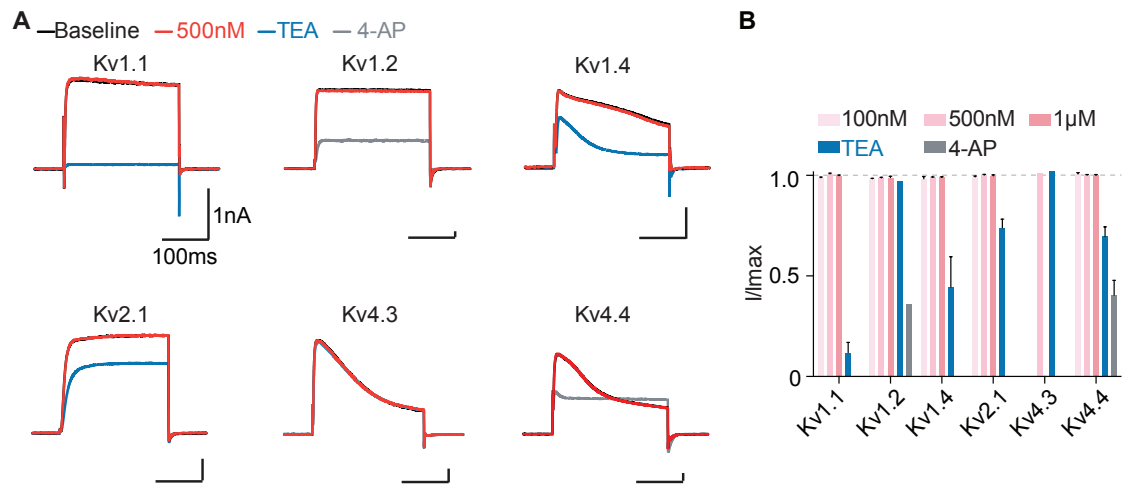Sm1a/Charybdotoxin

Figure. 13 Screen of synthetic Sm1a on potassium channels

(A) Whole-cell electrophysiology recording on HEK293 cells expressing different Kv channels. Holding potential, -80mV; voltage step +20mV. Vertical scale bars, 1nA; horizontal bars, 100ms. (B) Quantification of different Sm1a concentrations on Kv channels. Note that Sm1a has no effects in any of the tested Kv channels.

A

Baseline   500nM   TEA   4-AP

Kv1.1   Kv1.2   Kv1.4

1nA
100ms

Kv2.1   Kv4.3   Kv4.4

B

100nM   500nM   1μM
TEA   4-AP

1.0

I/Imax

0.5

0

Kv1.1 Kv1.2 Kv1.4 Kv2.1 Kv4.3 Kv4.4

Acknowledgement

Contributions

CHAPTER 5

Future Directions

Search for BomoTx receptor

The question concerning the nature of a Lys49 myotoxin receptor remains a major unanswered question in this field (Gutierrez and Lomonte 2013). This study has not tested specific candidates, but it is possible to set up a system using BomoTx to screen for candidates based on function.

Based on our current hypothesis, BomoTx targets a subpopulation of somatosensory neurons that express a potential receptor for the toxin. Upon binding the receptor, a PLC-mediated calcium signaling cascade is activated, which eventually leads to pannexin opening and ATP release. Since neurons expressing BomoTx receptors only represent about 5% of the total somatosensory neurons, it poses a big challenge to identify the receptor using traditional cDNA library expression cloning strategies that have been used to elucidate targets of capsaicin (more than 30% total neurons) and menthol (more than 15% total neurons). The problem lies in that the transcripts corresponding to the BomoTx receptor may not be highly represented in the total sensory neuron cDNA library, thus significantly increasing the signal to noise ratio. Similarly, single-cell transcriptome analysis between toxin responsive and non-responsive cells can also be challenging for the same reason of low abundance of toxin-responsive neurons.

Another strategy is to search for BomoTx receptors in a different system where they are more highly represented. Previous studies have shown that Lys49 myotoxins can cause specific calcium increase and ATP release in C2C12 myotubes but not C2C12

86

myoblast, indicating potential expression of a toxin receptor during C2C12 differentiation. We have also tested BomoTx on C2C12 cell lines and observed similar results: BomoTx shows no effect on C2C12 myoblasts but triggers calcium responses in C2C12 myotubes, while both respond to ATP due to the expression of endogenous ATP receptors (Figure. 14). Hence, we can utilize the C2C12 cell line and compare the transcriptomes before and after differentiation to search for genes that are highly expressed in myotubes. In addition, it is important to investigate whether myotube BomoTx responses show similar properties to neurons, including intracellular calcium release and PLC coupling. Since this model is consistent with a G-protein-coupled receptor or receptor tyrosine kinase pathway, we could narrow down candidate genes that belong to these categories.

Synthetic Sm1a target screen

In this study, we have identified a novel family of CSαβ centipede toxins that show structural similarity to defensins and scorpion α-KTxs. What has not been resolved, however, is the identity of target by this family of centipede toxins. Based on sequence analysis, Sm1a has many conserved residues that are required for potassium channel blocking in α-KTxs. We thus hypothesize that Sm1a potentially targets potassium channels. In order to test the channel candidates, we can use electrophysiology on HEK293 cells that heterologously express channels genes. In this study, a few members of the Kv families have been tested, but none show effects by Sm1a. In order to search for Sm1a targets, a much broader screen should be conducted that includes more members of the Kv families. In addition, as some of the α-KTxs have been

reported to inhibit calcium channels (Rodriguez de la Vega and Possani 2004), other channels families should also be tested.

Even though more work has to be done to elucidate whether native Sm1a faction contains other components that activate somatosensory neurons, this screen could potentially provide clues to the functional roles that Sm1a and its toxin family play, which could be tested again in sensory neurons.

Figure. 14 BomoTx activates C2C12 myotubes

(A-B) Calcium imaging traces of BomoTx on C2C12 myoblast (A) and differentiated myotubes (B). Subsequent response to ATP (100µM) reveals all cells in the field. Each trace represents an individual cell. Grey traces are non-responding cells; green traces are responding cells showing transient calcium responses; blue are responding cells showing sustained calcium responses.

A Myoblast
BomoTx   ATP

F_{340}/F_{380}
1.7
1.6
1.5
1.4
1.3
1.2
1.1

0   50   100   150
Time (s)

B Myotube
BomoTx   ATP

F_{340}/F_{380}
3.0
2.5
2.0
1.5
1.0

0   50   100
Time (s)
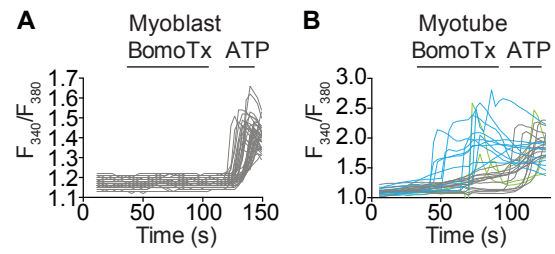
REFERENCES

Arcuino, G., J. H. Lin, T. Takano, C. Liu, L. Jiang, Q. Gao, J. Kang and M. Nedergaard (2002). "Intercellular calcium signaling mediated by point-source burst release of ATP." Proc Natl Acad Sci U S A **99**(15): 9840-9845.

Baconguis, I., C. J. Bohlen, A. Goehring, D. Julius and E. Gouaux (2014). "X-ray structure of acid-sensing ion channel 1-snake toxin complex reveals open state of a Na(+)-selective channel." Cell **156**(4): 717-729.

Balit, C. R., M. S. Harvey, J. M. Waldock and G. K. Isbister (2004). "Prospective study of centipede bites in Australia." J Toxicol Clin Toxicol **42**(1): 41-48.

Bao, L., S. Locovei and G. Dahl (2004). "Pannexin membrane channels are mechanosensitive conduits for ATP." FEBS Lett **572**(1-3): 65-68.

Basbaum, A. I., D. M. Bautista, G. Scherrer and D. Julius (2009). "Cellular and molecular mechanisms of pain." Cell **139**(2): 267-284.

Basbaum, A. I. and T. M. Jessell (2000). The perception of pain. Principles of Neural Science. J. S. ER Kandel, TM Jessell. New York, McGraw-Hill**:** 472-491.

Bautista, D. M., J. Siemens, J. M. Glazer, P. R. Tsuruda, A. I. Basbaum, C. L. Stucky, S. E. Jordt and D. Julius (2007). "The menthol receptor TRPM8 is the principal detector of environmental cold." Nature **448**(7150): 204-208.

Belmonte, G., L. Cescatti, B. Ferrari, T. Nicolussi, M. Ropele and G. Menestrina (1987). "Pore formation by Staphylococcus aureus alpha-toxin in lipid bilayers. Dependence upon temperature and toxin concentration." Eur Biophys J **14**(6): 349-358.

Bernardes, C. P., N. A. Santos-Filho, T. R. Costa, M. S. Gomes, F. S. Torres, J. Costa, M. H. Borges, M. Richardson, D. M. dos Santos, A. M. de Castro Pimenta, M. I. Homsi-Brandeburgo, A. M. Soares and F. de Oliveira (2008). "Isolation and structural characterization of a new fibrin(ogen)olytic metalloproteinase from Bothrops moojeni snake venom." Toxicon **51**(4): 574-584.

Bland-Ward, P. A. and P. P. Humphrey (1997). "Acute nociception mediated by hindpaw P2X receptor activation in the rat." Br J Pharmacol **122**(2): 365-371.

Bohlen, C. J., A. T. Chesler, R. Sharif-Naeini, K. F. Medzihradszky, S. Zhou, D. King, E. E. Sanchez, A. L. Burlingame, A. I. Basbaum and D. Julius (2011). "A heteromeric Texas coral snake toxin targets acid-sensing ion channels to produce pain." Nature **479**(7373): 410-414.

Bohlen, C. J., A. Priel, S. Zhou, D. King, J. Siemens and D. Julius (2010). "A bivalent tarantula toxin activates the capsaicin receptor, TRPV1, by targeting the outer pore domain." Cell **141**(5): 834-845.

Brunger, A. T. (2007). "Version 1.2 of the Crystallography and NMR system." Nat Protoc **2**(11): 2728-2733.

Buczek, O., D. Yoshikami, G. Bulaj, E. C. Jimenez and B. M. Olivera (2005). "Post-translational amino acid isomerization: a functionally important D-amino acid in an excitatory peptide." J Biol Chem **280**(6): 4247-4253.

Campbell, J. A., W. W. Lamar and E. D. Brodie (2004). The venomous reptiles of the Western Hemisphere. Ithaca N.Y., Comstock Pub. Associates.

Cao, E., M. Liao, Y. Cheng and D. Julius (2013). "TRPV1 structures in distinct conformations reveal activation mechanisms." Nature **504**(7478): 113-118.

Cao, Y. Q., P. W. Mantyh, E. J. Carlson, A. M. Gillespie, C. J. Epstein and A. I. Basbaum (1998). "Primary afferent tachykinins are required to experience moderate to intense pain." Nature **392**(6674): 390-394.

Casewell, N. R., W. Wuster, F. J. Vonk, R. A. Harrison and B. G. Fry (2013). "Complex cocktails: the evolutionary novelty of venoms." Trends Ecol Evol **28**(4): 219-229.

Cavanaugh, D. J., H. Lee, L. Lo, S. D. Shields, M. J. Zylka, A. I. Basbaum and D. J. Anderson (2009). "Distinct subsets of unmyelinated primary sensory fibers mediate behavioral responses to noxious thermal and mechanical stimuli." Proc Natl Acad Sci U S A **106**(22): 9075-9080.

Chahl, L. A. and E. J. Kirk (1975). "Toxins which produce pain." Pain **1**(1): 3-49.

Chakraborti, S. (2003). "Phospholipase A(2) isoforms: a perspective." Cell Signal **15**(7): 637-665.

Chekeni, F. B., M. R. Elliott, J. K. Sandilos, S. F. Walk, J. M. Kinchen, E. R. Lazarowski, A. J. Armstrong, S. Penuela, D. W. Laird, G. S. Salvesen, B. E. Isakson, D. A. Bayliss and K. S. Ravichandran (2010). "Pannexin 1 channels mediate 'find-me' signal release and membrane permeability during apoptosis." Nature **467**(7317): 863-867.

Chen, V. B., W. B. Arendall, 3rd, J. J. Headd, D. A. Keedy, R. M. Immormino, G. J. Kapral, L. W. Murray, J. S. Richardson and D. C. Richardson (2010). "MolProbity: all-atom structure validation for macromolecular crystallography." Acta Crystallogr D Biol Crystallogr **66**(Pt 1): 12-21.

Cintra-Francischinelli, M., P. Caccin, A. Chiavegato, P. Pizzo, G. Carmignoto, Y. Angulo, B. Lomonte, J. M. Gutierrez and C. Montecucco (2010). "Bothrops snake myotoxins induce a large efflux of ATP and potassium with spreading of cell damage and pain." Proc Natl Acad Sci U S A **107**(32): 14140-14145.

Cintra-Francischinelli, M., P. Pizzo, Y. Angulo, J. M. Gutierrez, C. Montecucco and B. Lomonte (2010). "The C-terminal region of a Lys49 myotoxin mediates Ca2+ influx in C2C12 myotubes." Toxicon **55**(2-3): 590-596.

Cintra-Francischinelli, M., P. Pizzo, L. Rodrigues-Simioni, L. A. Ponce-Soto, O. Rossetto, B. Lomonte, J. M. Gutierrez, T. Pozzan and C. Montecucco (2009). "Calcium imaging of muscle cells treated with snake myotoxins reveals toxin synergism and presence of acceptors." Cell Mol Life Sci **66**(10): 1718-1728.

Cockayne, D. A., P. M. Dunn, Y. Zhong, W. Rong, S. G. Hamilton, G. E. Knight, H. Z. Ruan, B. Ma, P. Yip, P. Nunn, S. B. McMahon, G. Burnstock and A. P. Ford (2005). "P2X2 knockout mice and P2X2/P2X3 double knockout mice reveal a role for the P2X2 receptor subunit in mediating multiple sensory effects of ATP." J Physiol **567**(Pt 2): 621-639.

Cockayne, D. A., S. G. Hamilton, Q. M. Zhu, P. M. Dunn, Y. Zhong, S. Novakovic, A. B. Malmberg, G. Cain, A. Berson, L. Kassotakis, L. Hedley, W. G. Lachnit, G. Burnstock, S. B. McMahon and A. P. Ford (2000). "Urinary bladder hyporeflexia and reduced pain-related behaviour in P2X3-deficient mice." Nature **407**(6807): 1011-1015.

Condrea, E., J. E. Fletcher, B. E. Rapuano, C. C. Yang and P. Rosenberg (1981). "Dissociation of enzymatic activity from lethality and pharmacological properties by carbamylation of lysines in Naja nigricollis and Naja naja atra snake venom phospholipases A2." Toxicon **19**(5): 705-720.

Coste, B., J. Mathur, M. Schmidt, T. J. Earley, S. Ranade, M. J. Petrus, A. E. Dubin and A. Patapoutian (2010). "Piezo1 and Piezo2 are essential components of distinct mechanically activated cation channels." Science **330**(6000): 55-60.

Cotrina, M. L., J. H. Lin, J. C. Lopez-Garcia, C. C. Naus and M. Nedergaard (2000). "ATP-mediated glia signaling." J Neurosci **20**(8): 2835-2844.

Dahl, G. (2015). "ATP release through pannexon channels." Philos Trans R Soc Lond B Biol Sci **370**(1672).

de Oliveira, F., B. B. de Sousa, C. C. Mamede, N. C. de Morais, M. R. de Queiroz, D. F. da Cunha Pereira, M. S. Matias and M. I. Homi Brandeburgo (2016). "Biochemical and functional characterization of BmooSP, a new serine protease from Bothrops moojeni snake venom." Toxicon **111**: 130-138.

Diochot, S., A. Baron, M. Salinas, D. Douguet, S. Scarzello, A. S. Dabert-Gay, D. Debayle, V. Friend, A. Alloui, M. Lazdunski and E. Lingueglia (2012). "Black mamba venom peptides target acid-sensing ion channels to abolish pain." Nature **490**(7421): 552-555.

Fernandes, C. A., R. J. Borges, B. Lomonte and M. R. Fontes (2014). "A structure-based proposal for a comprehensive myotoxic mechanism of phospholipase A2-like proteins from viperid snake venoms." Biochim Biophys Acta **1844**(12): 2265-2276.

Fernandez, J., P. Caccin, G. Koster, B. Lomonte, J. M. Gutierrez, C. Montecucco and A. D. Postle (2013). "Muscle phospholipid hydrolysis by Bothrops asper Asp49 and Lys49 phospholipase A(2) myotoxins--distinct mechanisms of action." FEBS J **280**(16): 3878-3886.

Franca, S. C., S. Kashima, P. G. Roberto, M. Marins, F. K. Ticli, J. O. Pereira, S. Astolfi-Filho, R. G. Stabeli, A. J. Magro, M. R. Fontes, S. V. Sampaio and A. M. Soares (2007). "Molecular approaches for structural characterization of Bothrops L-amino acid oxidases with antiprotozoal activity: cDNA cloning, comparative sequence analysis, and molecular modeling." Biochem Biophys Res Commun **355**(2): 302-306.

Fry, B. G., K. Roelants, D. E. Champagne, H. Scheib, J. D. Tyndall, G. F. King, T. J. Nevalainen, J. A. Norman, R. J. Lewis, R. S. Norton, C. Renjifo and R. C. de la Vega (2009). "The toxicogenomic multiverse: convergent recruitment of proteins into animal venoms." Annual review of genomics and human genetics **10**: 483-511.

Giannotti, K. C., E. Leiguez, V. Moreira, N. G. Nascimento, B. Lomonte, J. M. Gutierrez, R. Lopes de Melo and C. Teixeira (2013). "A Lys49 phospholipase A2, isolated from Bothrops asper snake venom, induces lipid droplet formation in macrophages which depends on distinct signaling pathways and the C-terminal region." Biomed Res Int **2013**: 807982.

Gutierrez, J. M. and B. Lomonte (1995). "Phospholipase A2 myotoxins from Bothrops snake venoms." Toxicon **33**(11): 1405-1424.

Gutierrez, J. M. and B. Lomonte (2013). "Phospholipases A2: unveiling the secrets of a functionally versatile group of snake venom toxins." Toxicon **62**: 27-39.

Gutierrez, J. M., B. Lomonte and L. Cerdas (1986). "Isolation and partial characterization of a myotoxin from the venom of the snake Bothrops nummifer." Toxicon **24**(9): 885-894.

Honore, P., K. Kage, J. Mikusa, A. T. Watt, J. F. Johnston, J. R. Wyatt, C. R. Faltynek, M. F. Jarvis and K. Lynch (2002). "Analgesic profile of intrathecal P2X(3) antisense oligonucleotide treatment in chronic inflammatory and neuropathic pain states in rats." Pain **99**(1-2): 11-19.

Idzko, M., D. Ferrari and H. K. Eltzschig (2014). "Nucleotide signalling during inflammation." Nature **509**(7500): 310-317.

Jahangir, A., M. Alam, D. S. Carter, M. P. Dillon, D. J. Bois, A. P. Ford, J. R. Gever, C. Lin, P. J. Wagner, Y. Zhai and J. Zira (2009). "Identification and SAR of novel diaminopyrimidines. Part 2: The discovery of RO-51, a potent and selective, dual P2X(3)/P2X(2/3) antagonist for the treatment of pain." Bioorg Med Chem Lett **19**(6): 1632-1635.

Julius, D. (2013). "TRP channels and pain." Annu Rev Cell Dev Biol **29**: 355-384.

Julius, D. and A. I. Basbaum (2001). "Molecular mechanisms of nociception." Nature **413**(6852): 203-210.

Khakh, B. S. (2001). "Molecular physiology of P2X receptors and ATP signalling at synapses." Nat Rev Neurosci **2**(3): 165-174.

King, G. F. (2011). "Venoms as a platform for human drugs: translating toxins into therapeutics." Expert Opin Biol Ther **11**(11): 1469-1484.

Kini, R. M. and H. J. Evans (1989). "A model to explain the pharmacological effects of snake venom phospholipases A2." Toxicon **27**(6): 613-635.

Lambeau, G. and M. Lazdunski (1999). "Receptors for a growing family of secreted phospholipases A2." Trends Pharmacol Sci **20**(4): 162-170.

Lambeau, G., A. Schmid-Alliana, M. Lazdunski and J. Barhanin (1990). "Identification and purification of a very high affinity binding protein for toxic phospholipases A2 in skeletal muscle." J Biol Chem **265**(16): 9526-9532.

Landon, C., P. Sodano, C. Hetru, J. Hoffmann and M. Ptak (1997). "Solution structure of drosomycin, the first inducible antifungal protein from insects." Protein Sci **6**(9): 1878-1884.

Lewallen, K. A., Y. A. Shen, A. R. De la Torre, B. K. Ng, D. Meijer and J. R. Chan (2011). "Assessing the role of the cadherin/catenin complex at the Schwann cell-axon interface and in the initiation of myelination." J Neurosci **31**(8): 3032-3043.

Lewis, C., S. Neidhart, C. Holy, R. A. North, G. Buell and A. Surprenant (1995). "Coexpression of P2X2 and P2X3 receptor subunits can account for ATP-gated currents in sensory neurons." Nature **377**(6548): 432-435.

Liu, Z. C., R. Zhang, F. Zhao, Z. M. Chen, H. W. Liu, Y. J. Wang, P. Jiang, Y. Zhang, Y. Wu, J. P. Ding, W. H. Lee and Y. Zhang (2012). "Venomic and transcriptomic analysis of centipede Scolopendra subspinipes dehaani." J Proteome Res **11**(12): 6197-6212.

Lomonte, B., Y. Angulo, S. Rufini, W. Cho, J. R. Giglio, M. Ohno, J. J. Daniele, P. Geoghegan and J. M. Gutierrez (1999). "Comparative study of the cytolytic activity of myotoxic phospholipases A2 on mouse endothelial (tEnd) and skeletal muscle (C2C12) cells in vitro." Toxicon **37**(1): 145-158.

Lomonte, B. and J. Rangel (2012). "Snake venom Lys49 myotoxins: From phospholipases A(2) to non-enzymatic membrane disruptors." Toxicon **60**(4): 520-530.

Luna-Ramirez, K., A. Bartok, R. Restano-Cassulini, V. Quintero-Hernandez, F. I. Coronas, J. Christensen, C. E. Wright, G. Panyi and L. D. Possani (2014). "Structure, molecular modeling, and function of the novel potassium channel blocker urotoxin isolated from the venom of the Australian scorpion Urodacus yaschenkoi." Mol Pharmacol **86**(1): 28-41.

MacVicar, B. A. and R. J. Thompson (2010). "Non-junction functions of pannexin-1 channels." Trends Neurosci **33**(2): 93-102.

Maraganore, J. M., G. Merutka, W. Cho, W. Welches, F. J. Kezdy and R. L. Heinrikson (1984). "A new class of phospholipases A2 with lysine in place of aspartate 49. Functional consequences for calcium and substrate binding." J Biol Chem **259**(22): 13839-13843.

Meng, L., Z. Xie, Q. Zhang, Y. Li, F. Yang, Z. Chen, W. Li, Z. Cao and Y. Wu (2016). "Scorpion Potassium Channel-blocking Defensin Highlights a Functional Link with Neurotoxin." J Biol Chem **291**(13): 7097-7106.

Miller, C. (1995). "The charybdotoxin family of K+ channel-blocking peptides." Neuron **15**(1): 5-10.

Mishra, S. K. and M. A. Hoon (2010). "Ablation of TrpV1 neurons reveals their selective role in thermal pain sensation." Mol Cell Neurosci **43**(1): 157-163.

Montecucco, C., J. M. Gutierrez and B. Lomonte (2008). "Cellular pathology induced by snake venom phospholipase A2 myotoxins and neurotoxins: common aspects of their mechanisms of action." Cell Mol Life Sci **65**(18): 2897-2912.

Moreira, V., P. C. de Castro Souto, M. A. Ramirez Vinolo, B. Lomonte, J. Maria Gutierrez, R. Curi and C. Teixeira (2013). "A catalytically-inactive snake venom Lys49 phospholipase A(2) homolog induces expression of cyclooxygenase-2 and production of prostaglandins through selected signaling pathways in macrophages." Eur J Pharmacol **708**(1-3): 68-79.

Nakashima, K., T. Ogawa, N. Oda, M. Hattori, Y. Sakaki, H. Kihara and M. Ohno (1993). "Accelerated evolution of Trimeresurus flavoviridis venom gland phospholipase A2 isozymes." Proc Natl Acad Sci U S A **90**(13): 5964-5968.

Nederveen, A. J., J. F. Doreleijers, W. Vranken, Z. Miller, C. A. Spronk, S. B. Nabuurs, P. Guntert, M. Livny, J. L. Markley, M. Nilges, E. L. Ulrich, R. Kaptein and A. M. Bonvin (2005). "RECOORD: a recalculated coordinate database of 500+ proteins from the PDB using restraints from the BioMagResBank." Proteins **59**(4): 662-672.

Nishioka, S. A., P. V. Silveira, F. M. Peixoto-Filho, M. T. Jorge and A. Sandoz (2000). "Occupational injuries with captive lance-headed vipers (Bothrops moojeni): experience from a snake farm in Brazil." Trop Med Int Health **5**(7): 507-510.

Nishioka Sde, A. and P. V. Silveira (1992). "A clinical and epidemiologic study of 292 cases of lance-headed viper bite in a Brazilian teaching hospital." Am J Trop Med Hyg **47**(6): 805-810.

North, R. A. (2002). "Molecular physiology of P2X receptors." Physiol Rev **82**(4): 1013-1067.

Osteen, J. D., V. Herzig, J. Gilchrist, J. J. Emrick, C. Zhang, X. Wang, J. Castro, S. Garcia-Caraballo, L. Grundy, G. Y. Rychkov, A. D. Weyer, Z. Dekan, E. A. Undheim, P. Alewood, C. L. Stucky, S. M. Brierley, A. I. Basbaum, F. Bosmans, G. F. King and D. Julius (2016). "Selective spider toxins reveal a role for the Nav1.1 channel in mechanical pain." Nature **534**(7608): 494-499.

Pankratov, Y., U. Lalo, A. Verkhratsky and R. A. North (2006). "Vesicular release of ATP at central synapses." Pflugers Arch **452**(5): 589-597.

Parfrey, L. W., D. J. Lahr, A. H. Knoll and L. A. Katz (2011). "Estimating the timing of early eukaryotic diversification with multigene molecular clocks." Proc Natl Acad Sci U S A **108**(33): 13624-13629.

Patapoutian, A., S. Tate and C. J. Woolf (2009). "Transient receptor potential channels: targeting pain at the source." Nat Rev Drug Discov **8**(1): 55-68.

Pinheiro, A. R., D. Paramos-de-Carvalho, M. Certal, C. Costa, M. T. Magalhaes-Cardoso, F. Ferreirinha, M. A. Costa and P. Correia-de-Sa (2013). "Bradykinin-induced

Ca2+ signaling in human subcutaneous fibroblasts involves ATP release via hemichannels leading to P2Y12 receptors activation." Cell Commun Signal **11**: 70.

Pinheiro, A. R., D. Paramos-de-Carvalho, M. Certal, M. A. Costa, C. Costa, M. T. Magalhaes-Cardoso, F. Ferreirinha, J. Sevigny and P. Correia-de-Sa (2013). "Histamine induces ATP release from human subcutaneous fibroblasts, via pannexin-1 hemichannels, leading to Ca2+ mobilization and cell proliferation." J Biol Chem **288**(38): 27571-27583.

Rabasseda, X., C. Solsona, J. Marsal, G. Egea and B. Bizzini (1987). "ATP release from pure cholinergic synaptosomes is not blocked by tetanus toxin." FEBS Lett **213**(2): 337-340.

Rigoni, M., P. Caccin, S. Gschmeissner, G. Koster, A. D. Postle, O. Rossetto, G. Schiavo and C. Montecucco (2005). "Equivalent effects of snake PLA2 neurotoxins and lysophospholipid-fatty acid mixtures." Science **310**(5754): 1678-1680.

Rodriguez de la Vega, R. C. and L. D. Possani (2004). "Current views on scorpion toxins specific for K+-channels." Toxicon **43**(8): 865-875.

Rodriguez de la Vega, R. C. and L. D. Possani (2005). "Overview of scorpion toxins specific for Na+ channels and related peptides: biodiversity, structure-function relationships and evolution." Toxicon **46**(8): 831-844.

Sartim, M. A., T. R. Costa, H. J. Laure, M. S. Espindola, F. G. Frantz, C. A. Sorgi, A. C. Cintra, E. C. Arantes, L. H. Faccioli, J. C. Rosa and S. V. Sampaio (2016).

"Moojenactivase, a novel pro-coagulant PIIId metalloprotease isolated from Bothrops moojeni snake venom, activates coagulation factors II and X and induces tissue factor up-regulation in leukocytes." Arch Toxicol **90**(5): 1261-1278.

Sawada, K., N. Echigo, N. Juge, T. Miyaji, M. Otsuka, H. Omote, A. Yamamoto and Y. Moriyama (2008). "Identification of a vesicular nucleotide transporter." Proc Natl Acad Sci U S A **105**(15): 5683-5686.

Seminario-Vidal, L., S. Kreda, L. Jones, W. O'Neal, J. Trejo, R. C. Boucher and E. R. Lazarowski (2009). "Thrombin promotes release of ATP from lung epithelial cells through coordinated activation of rho- and Ca2+-dependent signaling pathways." J Biol Chem **284**(31): 20638-20648.

Seminario-Vidal, L., S. F. Okada, J. I. Sesma, S. M. Kreda, C. A. van Heusden, Y. Zhu, L. C. Jones, W. K. O'Neal, S. Penuela, D. W. Laird, R. C. Boucher and E. R. Lazarowski (2011). "Rho signaling regulates pannexin 1-mediated ATP release from airway epithelia." J Biol Chem **286**(30): 26277-26286.

Shen, Y. and A. Bax (2013). "Protein backbone and sidechain torsion angles predicted from NMR chemical shifts using artificial neural networks." J Biomol NMR **56**(3): 227-241.

Siemens, J., S. Zhou, R. Piskorowski, T. Nikai, E. A. Lumpkin, A. I. Basbaum, D. King and D. Julius (2006). "Spider toxins activate the capsaicin receptor to produce inflammatory pain." Nature **444**(7116): 208-212.

Silveira, L. B., D. P. Marchi-Salvador, N. A. Santos-Filho, F. P. Silva, Jr., S. Marcussi, A. L. Fuly, A. Nomizo, S. L. da Silva, R. G. Stabeli, E. C. Arantes and A. M. Soares (2013). "Isolation and expression of a hypotensive and anti-platelet acidic phospholipase A2 from Bothrops moojeni snake venom." J Pharm Biomed Anal **73**: 35-43.

Skals, M., N. R. Jorgensen, J. Leipziger and H. A. Praetorius (2009). "Alpha-hemolysin from Escherichia coli uses endogenous amplification through P2X receptor activation to induce hemolysis." Proc Natl Acad Sci U S A **106**(10): 4030-4035.

Soares, A. M., S. H. Andriao-Escarso, Y. Angulo, B. Lomonte, J. M. Gutierrez, S. Marangoni, M. H. Toyama, R. K. Arni and J. R. Giglio (2000). "Structural and functional characterization of myotoxin I, a Lys49 phospholipase A(2) homologue from Bothrops moojeni (Caissaca) snake venom." Arch Biochem Biophys **373**(1): 7-15.

Sollod, B. L., D. Wilson, O. Zhaxybayeva, J. P. Gogarten, R. Drinkwater and G. F. King (2005). "Were arachnids the first to use combinatorial peptide libraries?" Peptides **26**(1): 131-139.

Song, J., B. Gilquin, N. Jamin, E. Drakopoulou, M. Guenneugues, M. Dauplais, C. Vita and A. Menez (1997). "NMR solution structure of a two-disulfide derivative of charybdotoxin: structural evidence for conservation of scorpion toxin alpha/beta motif and its hydrophobic side chain packing." Biochemistry **36**(13): 3760-3766.

Staikopoulos, V., B. J. Sessle, J. B. Furness and E. A. Jennings (2007). "Localization of P2X2 and P2X3 receptors in rat trigeminal ganglion neurons." Neuroscience **144**(1): 208-216.

Strong, P. N., J. Goerke, S. G. Oberg and R. B. Kelly (1976). "beta-Bungarotoxin, a pre-synaptic toxin with enzymatic activity." Proc Natl Acad Sci U S A **73**(1): 178-182.

Sugiarto, H. and P. L. Yu (2004). "Avian antimicrobial peptides: the defense role of beta-defensins." Biochem Biophys Res Commun **323**(3): 721-727.

Sunagar, K., E. A. Undheim, A. H. Chan, I. Koludarov, S. A. Munoz-Gomez, A. Antunes and B. G. Fry (2013). "Evolution stings: the origin and diversification of scorpion toxin peptide scaffolds." Toxins (Basel) **5**(12): 2456-2487.

Tonello, F., M. Simonato, A. Aita, P. Pizzo, J. Fernandez, B. Lomonte, J. M. Gutierrez and C. Montecucco (2012). "A Lys49-PLA2 myotoxin of Bothrops asper triggers a rapid death of macrophages that involves autocrine purinergic receptor signaling." Cell Death Dis **3**: e343.

Tsuda, M., S. Koizumi, A. Kita, Y. Shigemoto, S. Ueno and K. Inoue (2000). "Mechanical allodynia caused by intraplantar injection of P2X receptor agonist in rats: involvement of heteromeric P2X2/3 receptor signaling in capsaicin-insensitive primary afferent neurons." J Neurosci **20**(15): RC90.

Undheim, E. A., B. G. Fry and G. F. King (2015). "Centipede venom: recent discoveries and current state of knowledge." Toxins (Basel) **7**(3): 679-704.

Undheim, E. A., L. L. Grimm, C. F. Low, D. Morgenstern, V. Herzig, P. Zobel-Thropp, S. S. Pineda, R. Habib, S. Dziemborowicz, B. G. Fry, G. M. Nicholson, G. J. Binford, M. Mobli and G. F. King (2015). "Weaponization of a Hormone: Convergent Recruitment of Hyperglycemic Hormone into the Venom of Arthropod Predators." Structure **23**(7): 1283-1292.

Undheim, E. A., R. A. Jenner and G. F. King (2016). "Centipede venoms as a source of drug leads." Expert Opin Drug Discov **11**(12): 1139-1149.

Undheim, E. A., A. Jones, K. R. Clauser, J. W. Holland, S. S. Pineda, G. F. King and B. G. Fry (2014). "Clawing through evolution: toxin diversification and convergence in the ancient lineage Chilopoda (centipedes)." Mol Biol Evol **31**(8): 2124-2148.

Undheim, E. A. and G. F. King (2011). "On the venom system of centipedes (Chilopoda), a neglected group of venomous animals." Toxicon **57**(4): 512-524.

Undheim, E. A., M. Mobli and G. F. King (2016). "Toxin structures as evolutionary tools: Using conserved 3D folds to study the evolution of rapidly evolving peptides." Bioessays **38**(6): 539-548.

Undheim, E. A., K. Sunagar, B. R. Hamilton, A. Jones, D. J. Venter, B. G. Fry and G. F. King (2014). "Multifunctional warheads: diversification of the toxin arsenal of centipedes via novel multidomain transcripts." J Proteomics **102**: 1-10.

Valentin, E. and G. Lambeau (2000). "What can venom phospholipases A(2) tell us about the functional diversity of mammalian secreted phospholipases A(2)?" Biochimie **82**(9-10): 815-831.

Vetter, I., J. L. Davis, L. D. Rash, R. Anangi, M. Mobli, P. F. Alewood, R. J. Lewis and G. F. King (2011). "Venomics: a new paradigm for natural products-based drug discovery." Amino Acids **40**(1): 15-28.

Vranken, W. F., W. Boucher, T. J. Stevens, R. H. Fogh, A. Pajon, M. Llinas, E. L. Ulrich, J. L. Markley, J. Ionides and E. D. Laue (2005). "The CCPN data model for NMR spectroscopy: development of a software pipeline." Proteins **59**(4): 687-696.

Vriens, K., T. L. Cools, P. J. Harvey, D. J. Craik, A. Braem, J. Vleugels, B. De Coninck, B. P. Cammue and K. Thevissen (2016). "The radish defensins RsAFP1 and RsAFP2 act synergistically with caspofungin against Candida albicans biofilms." Peptides **75**: 71-79.

Ward, R. J., L. Chioato, A. H. de Oliveira, R. Ruller and J. M. Sa (2002). "Active-site mutagenesis of a Lys49-phospholipase A2: biological and membrane-disrupting activities in the absence of catalysis." Biochem J **362**(Pt 1): 89-96.

Wery, J. P., R. W. Schevitz, D. K. Clawson, J. L. Bobbitt, E. R. Dow, G. Gamboa, T. Goodson, Jr., R. B. Hermann, R. M. Kramer, D. B. McClure and et al. (1991). "Structure of recombinant human rheumatoid arthritic synovial fluid phospholipase A2 at 2.2 A resolution." Nature **352**(6330): 79-82.

Woolf, C. J. and Q. Ma (2007). "Nociceptors--noxious stimulus detectors." <u>Neuron</u> **55**(3): 353-364.

Wu, Y., B. Gao and S. Zhu (2017). "New fungal defensin-like peptides provide evidence for fold change of proteins in evolution." <u>Biosci Rep</u> **37**(1).

Yang, S., Z. Liu, Y. Xiao, Y. Li, M. Rong, S. Liang, Z. Zhang, H. Yu, G. F. King and R. Lai (2012). "Chemical punch packed in venoms makes centipedes excellent predators." <u>Mol Cell Proteomics</u> **11**(9): 640-650.

Yang, S., Y. Xiao, D. Kang, J. Liu, Y. Li, E. A. Undheim, J. K. Klint, M. Rong, R. Lai and G. F. King (2013). "Discovery of a selective NaV1.7 inhibitor from centipede venom with analgesic efficacy exceeding morphine in rodent pain models." <u>Proc Natl Acad Sci U S A</u> **110**(43): 17534-17539.

Yang, S., F. Yang, N. Wei, J. Hong, B. Li, L. Luo, M. Rong, V. Yarov-Yarovoy, J. Zheng, K. Wang and R. Lai (2015). "A pain-inducing centipede toxin targets the heat activation machinery of nociceptor TRPV1." <u>Nat Commun</u> **6**: 8297.
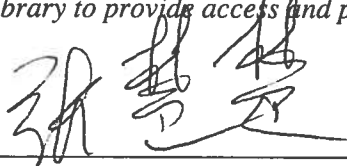
Zhang, X., Y. Chen, C. Wang and L. Y. Huang (2007). "Neuronal somatic ATP release triggers neuron-satellite glial cell communication in dorsal root ganglia." <u>Proc Natl Acad Sci U S A</u> **104**(23): 9864-9869.

Publishing Agreement

It is the policy of the University to encourage the distribution of all theses, dissertations, and manuscripts. Copies of all UCSF theses, dissertations, and manuscripts will be routed to the library via the Graduate Division. The library will make all theses, dissertations, and manuscripts accessible to the public and will preserve these to the best of their abilities, in perpetuity.

Please sign the following statement:

I hereby grant permission to the Graduate Division of the University of California, San Francisco to release copies of my thesis, dissertation, or manuscript to the Campus Library to provide access and preservation, in whole or in part, in perpetuity.

_____
Author Signature

3/17/2017
Date

111